Determination of Stellar Parameters and Chemical Abundances *in Solar Type Stars*

@DrJorgeMelendez,Univ. São Paulo, Brazil

Atmospheric physical parameters:

- Effective temperature (T_{eff})
- Surface gravity (log *g*)
- Metallicity ([Fe/H]: log of iron content in the star relative to the Sun)

Effective temperature

Solar flux f_d at distance d

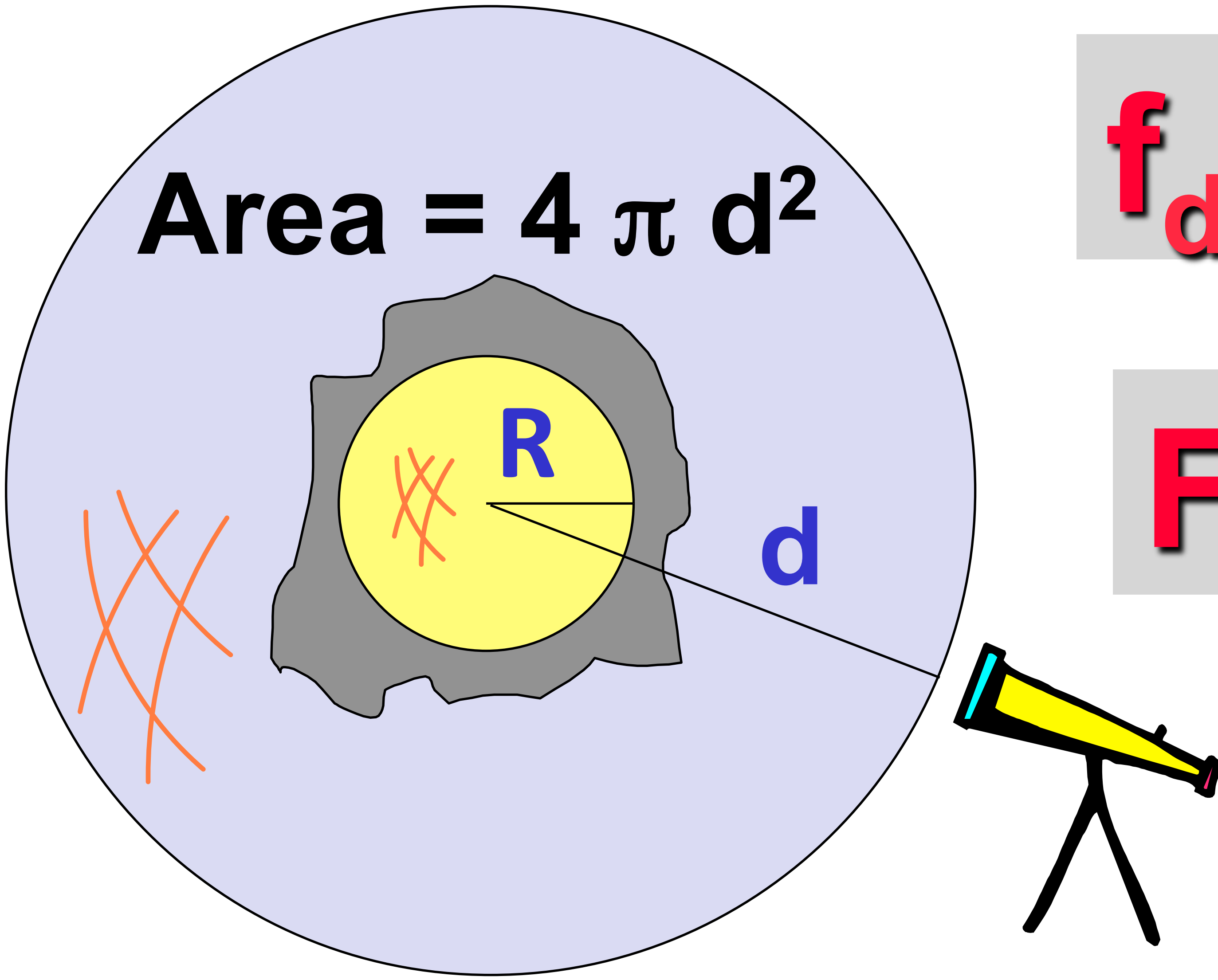

$$f_d = F_R \cdot R^2/d^2$$

$$F_R = f_d \cdot d^2/R^2$$

Sun's flux $\mathbf{f_d}$ at 1 A.U. (spectral irradiance)

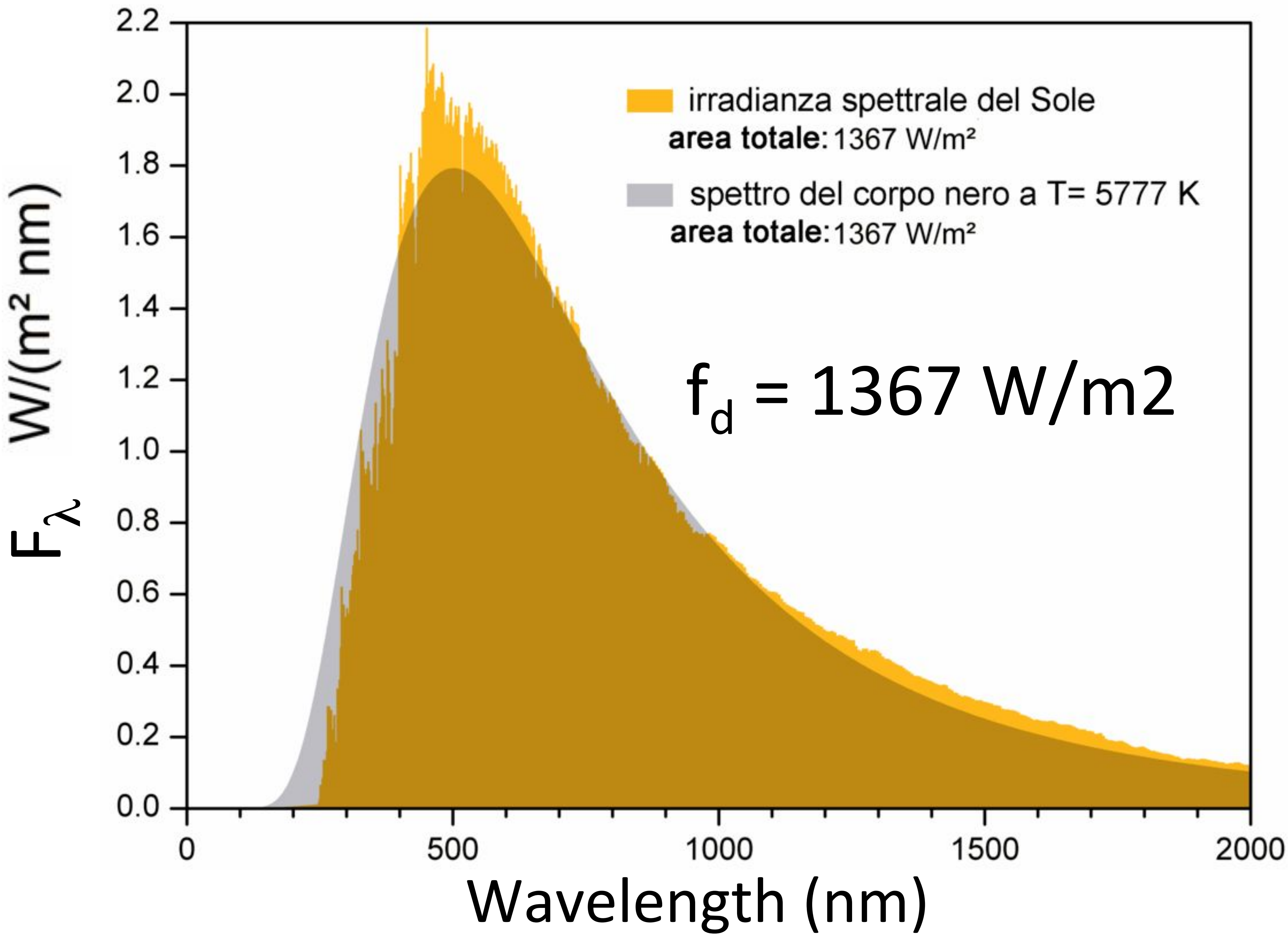

Effective temperature (T_{eff}): temperature corresponding to a black body with the same total flux *F* (at stellar surface)

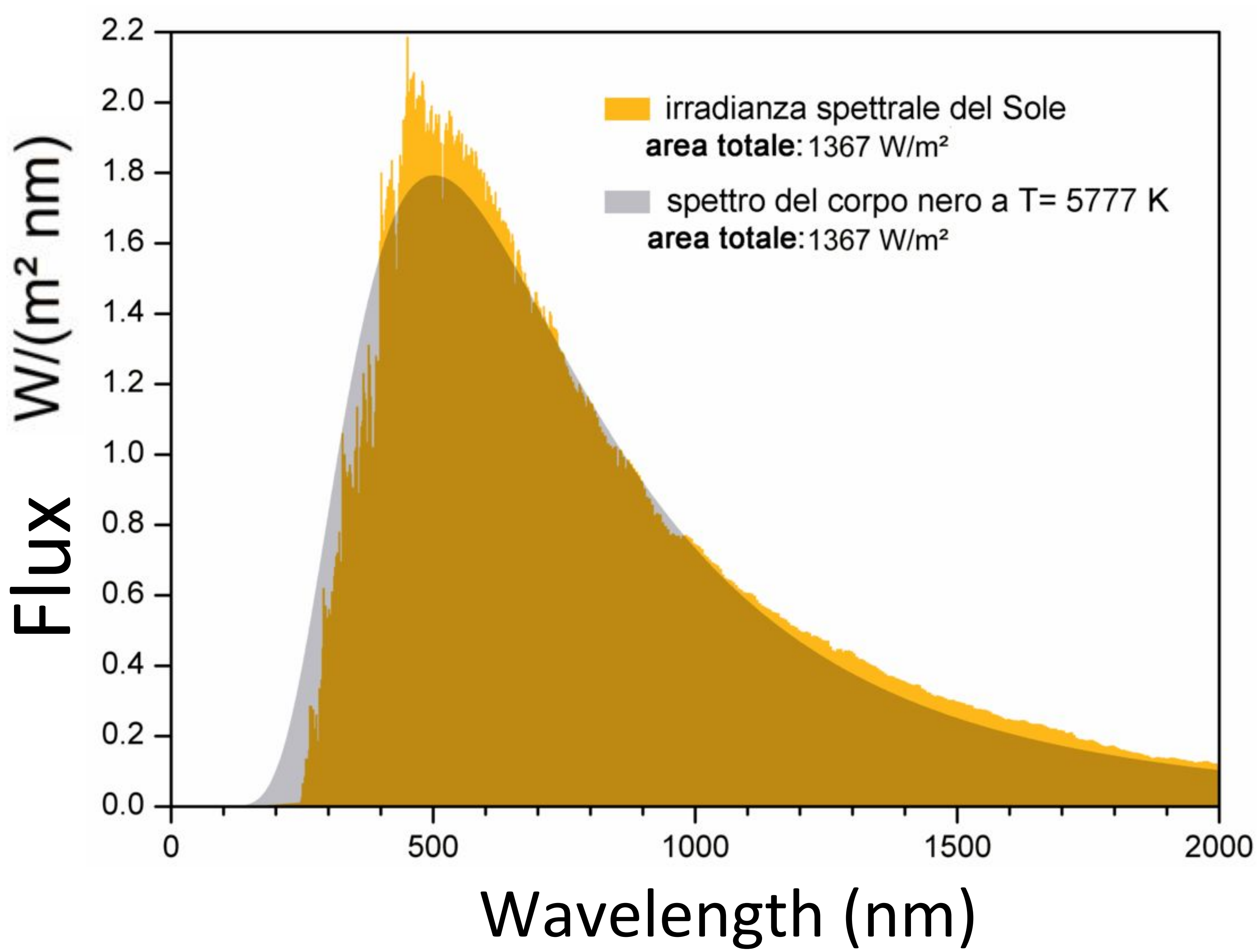

$$F = \sigma T_{eff}^{\ 4}$$

$$\mathbf{T_{eff}} = 5777\ \mathrm{K}$$

How to get T_{eff}?

$$L = 4\pi R^2 \sigma T_{eff}^4$$

$$L = 4\pi R^2 F = 4\pi d^2 f$$

R: stellar radius

r: distance Earth - star

θ: stellar angular diameter

f : flux measured at Earth

F: Flux at radius R

$\sigma = 5.67\times10^{-5}$ erg s^{-1} cm^{-2} K^{-4}

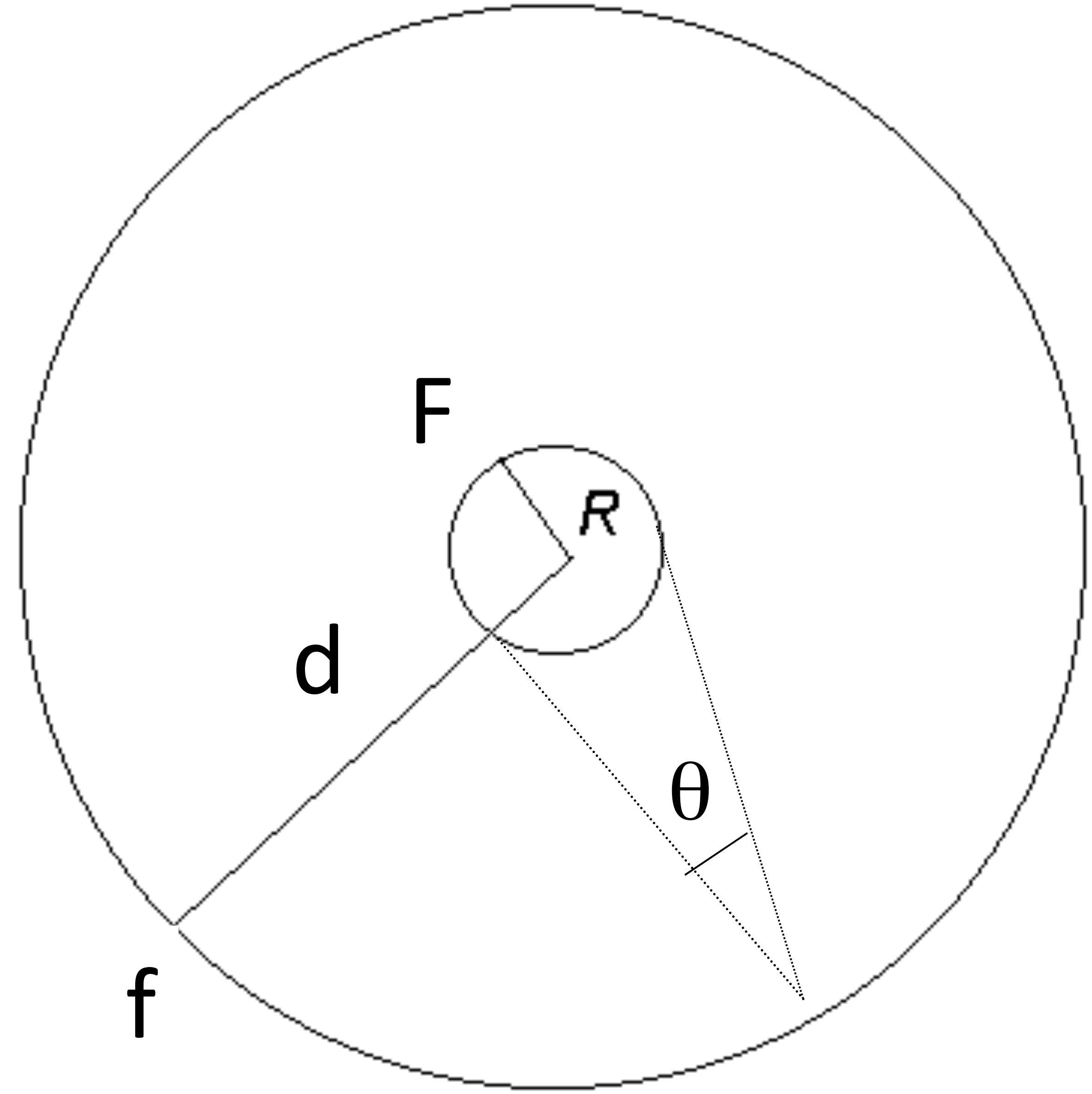

$$F = (R/d)^{-2} f$$

$$R/d = (\theta/2)$$

$$F = (\theta/2)^{-2} f$$

$$F = (\theta/2)^{-2} f$$

$$\sigma T_{eff}^4 = F$$

$$\sigma T_{eff}^4 = (\theta/2)^{-2} f$$

Angular diameter

Bolometric flux

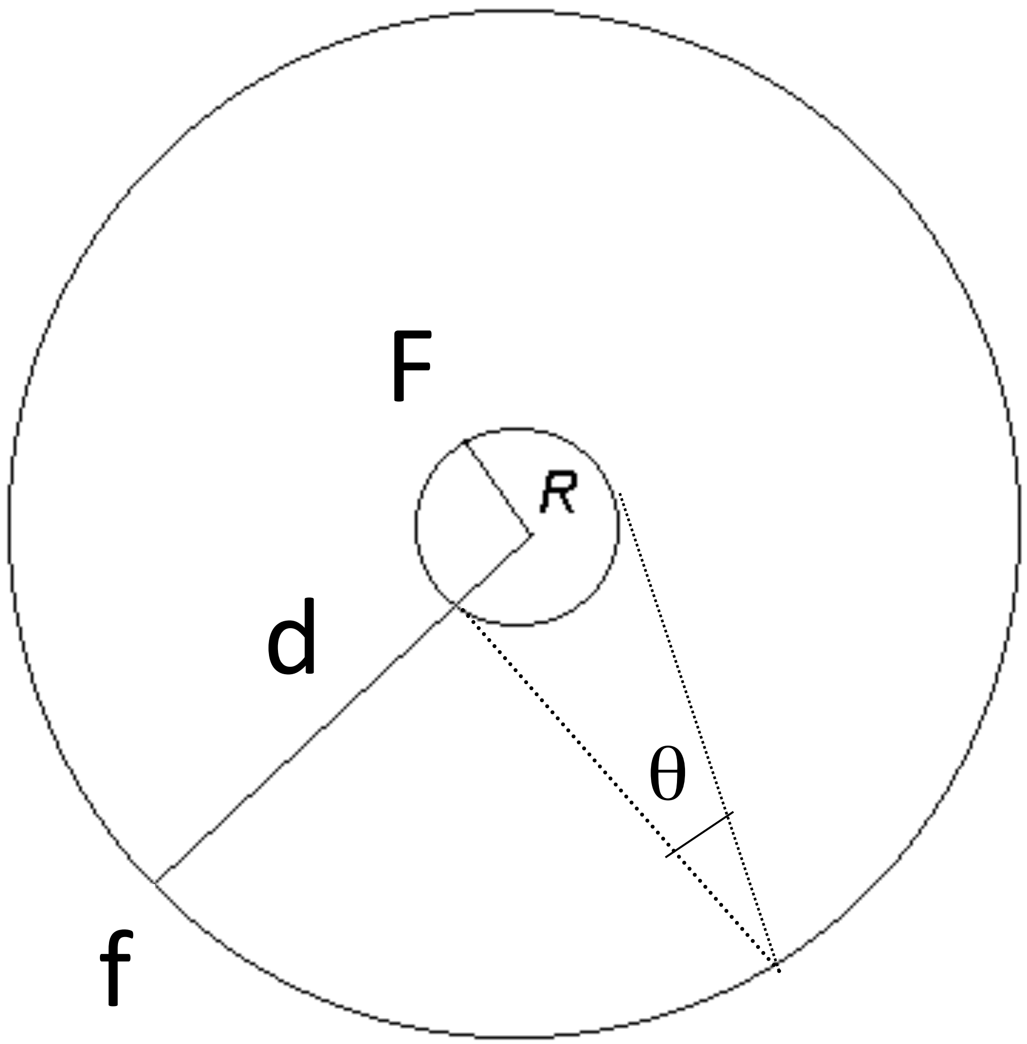

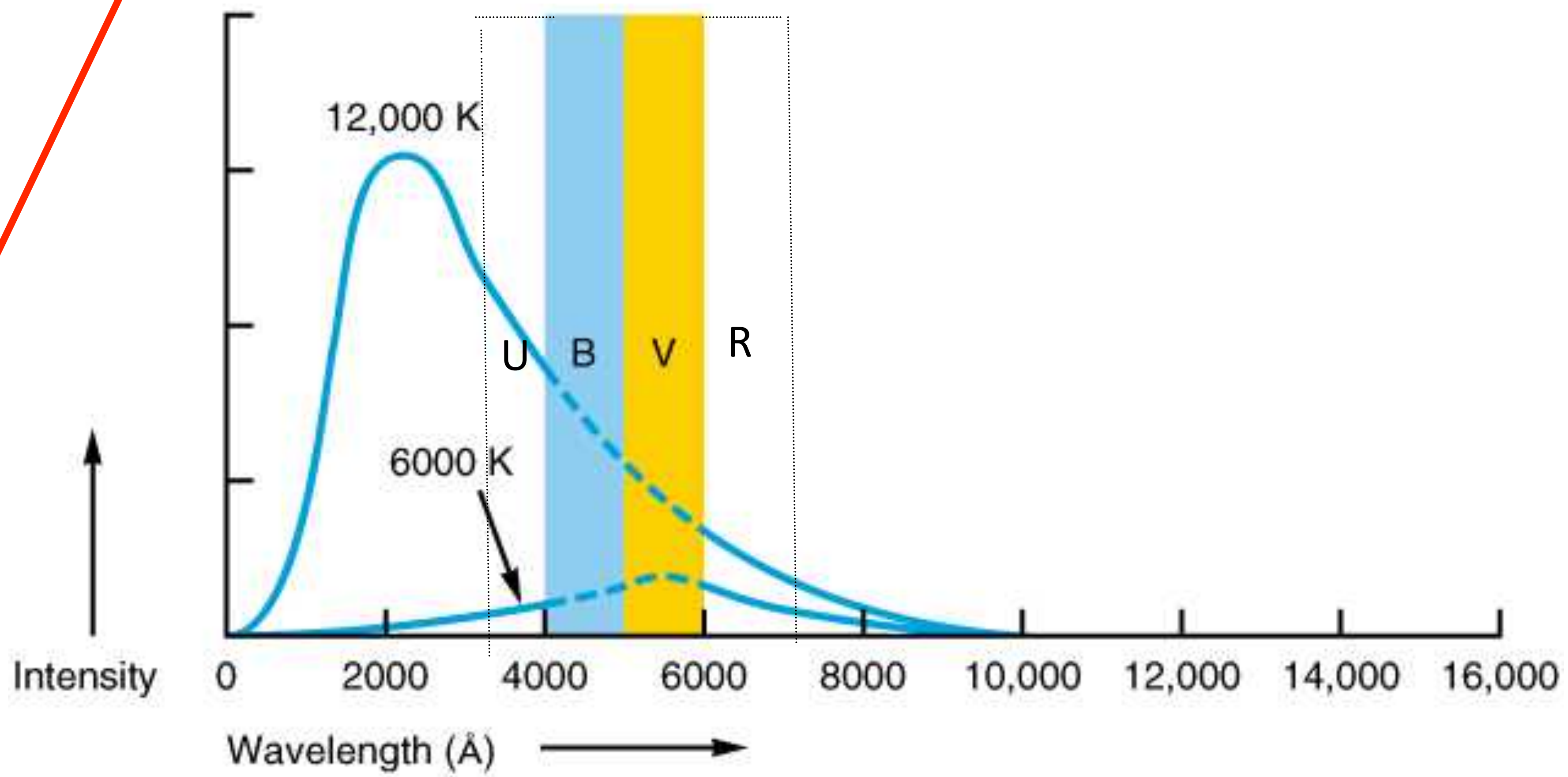

Angular diameter

$$\sigma T_{eff}^4 = (\theta/2)^{-2} f$$

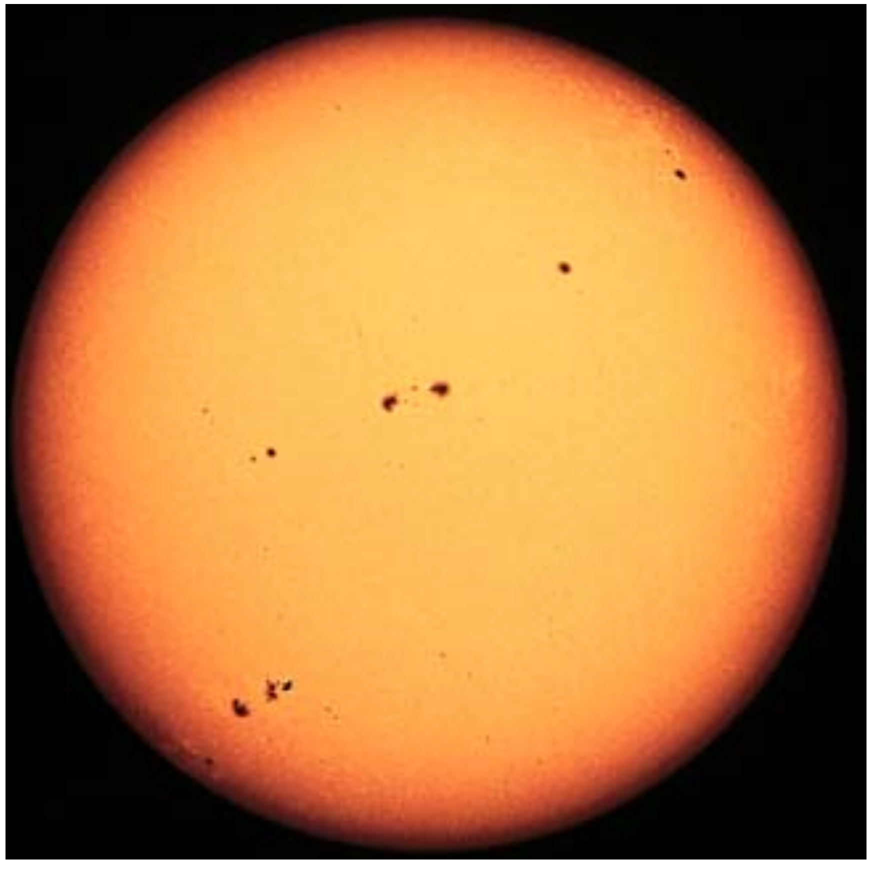

Sun

$\theta = 1919''.3$

Flux received: 1.371×10^6 erg cm^{-2} s^{-1} (*solar constant*)

$\Rightarrow T_{eff} = 5777$ K

α Lyrae

$\theta = 3 \times 10^{-3}$ ''

Bolometric flux (f_{bol}) ideally integrate total flux from measurements in several bands, otherwise measure at least in 1 band & use **B**ol. **C**orrection **BC**

774 *R. A. Bell, G. Paltoglou and M. J. Tripicco*

$m_{bol} = V + BC_V$

From $m_{bol} \rightarrow f_{bol}$ and then estimate T_{eff} (assuming you know angular diameter)

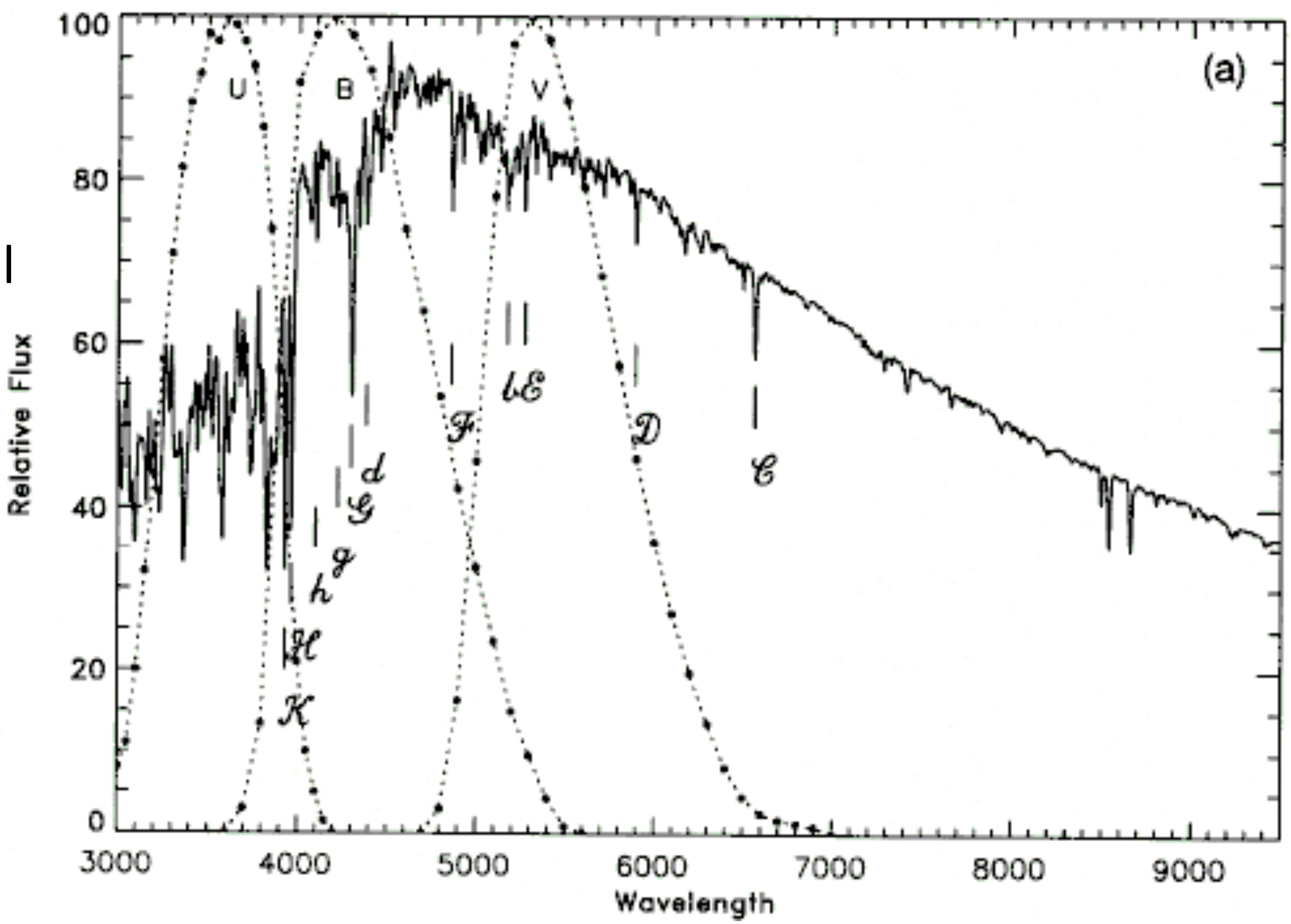

Don't know angular diameter?

Infrared Flux Method: IRFM

Blackwell & Shallis (1977),
Saxner & Hammarback (1985),
Alonso et al. (1996, 99)

$$\sigma T_{eff}^4 = (\theta/2)^{-2} f_{bol}$$

$$\theta/2 = R/d = (f / F)^{1/2}$$

$$(\theta/2)^{-2} = F / f = F_\lambda / f_\lambda$$

$$\sigma T_{eff}^4 = (F_\lambda / f_\lambda) f_{bol}$$

$$\sigma T_{eff}^4 = (F_{IR}/f_{IR}) f_{bol}$$

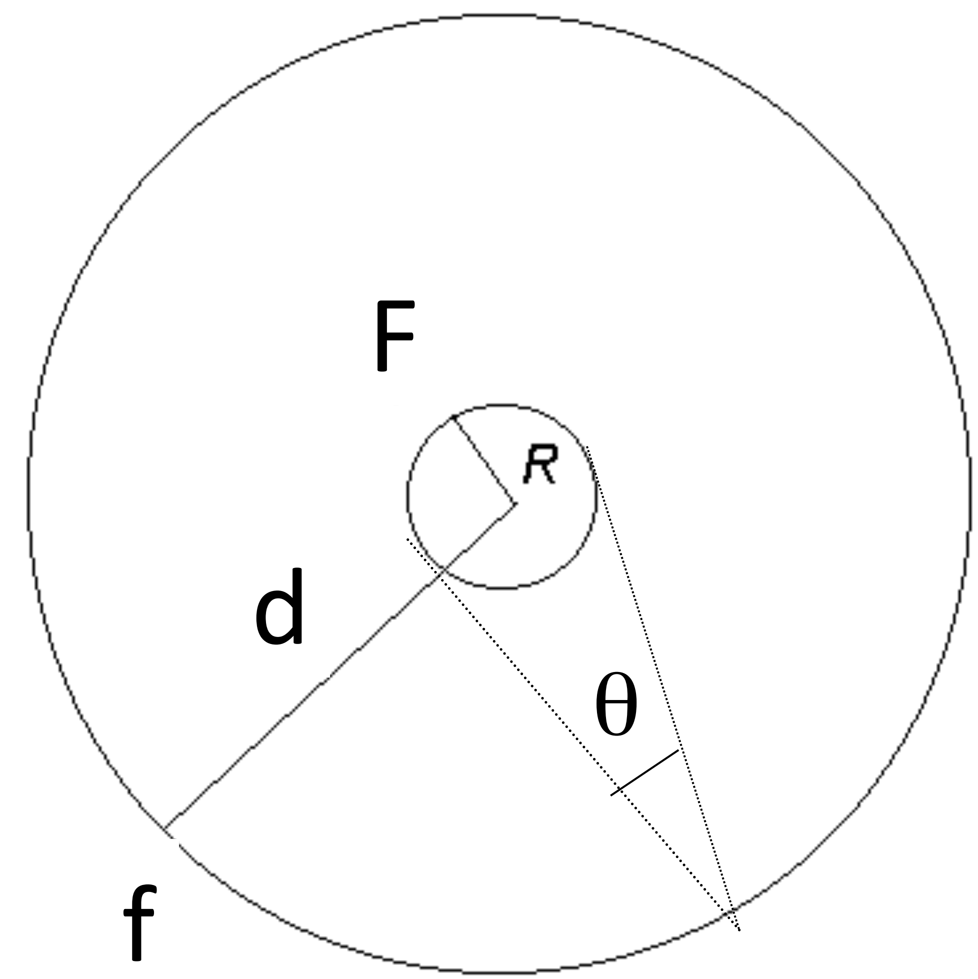

Synthetic (computed) infrared flux (e.g., K band) at stellar surface (at radius R)

Measured infrared flux (e.g. K band) on Earth

Bolometric flux at Earth (total flux from different bands, or using at least 1 band + BC)

In short, to apply the IRFM we required observations:

- Infrared photometry (e.g. 2MASS J, H, K_S)
- Bolometric flux (integrated flux using different bands)

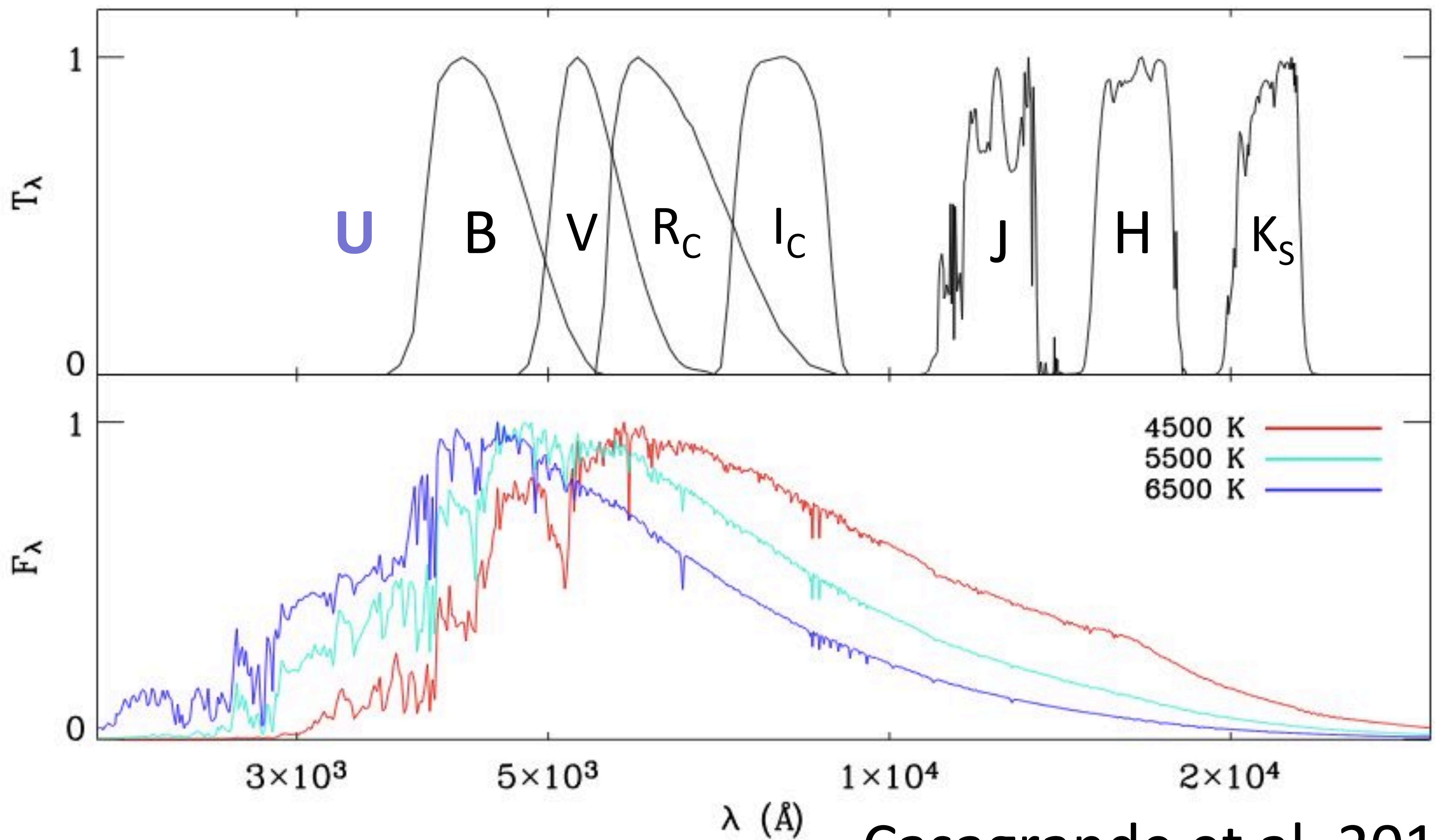

Casagrande et al. 2010

Model atmospheres broad-band colors, bolometric corrections and temperature calibrations for O - M stars*

M.S. Bessell[1], F. Castelli[2], and B. Plez[3,4]

Astron. Astrophys. 333, 231–250 (1998)

Another way to get T_{eff}: color calibrations

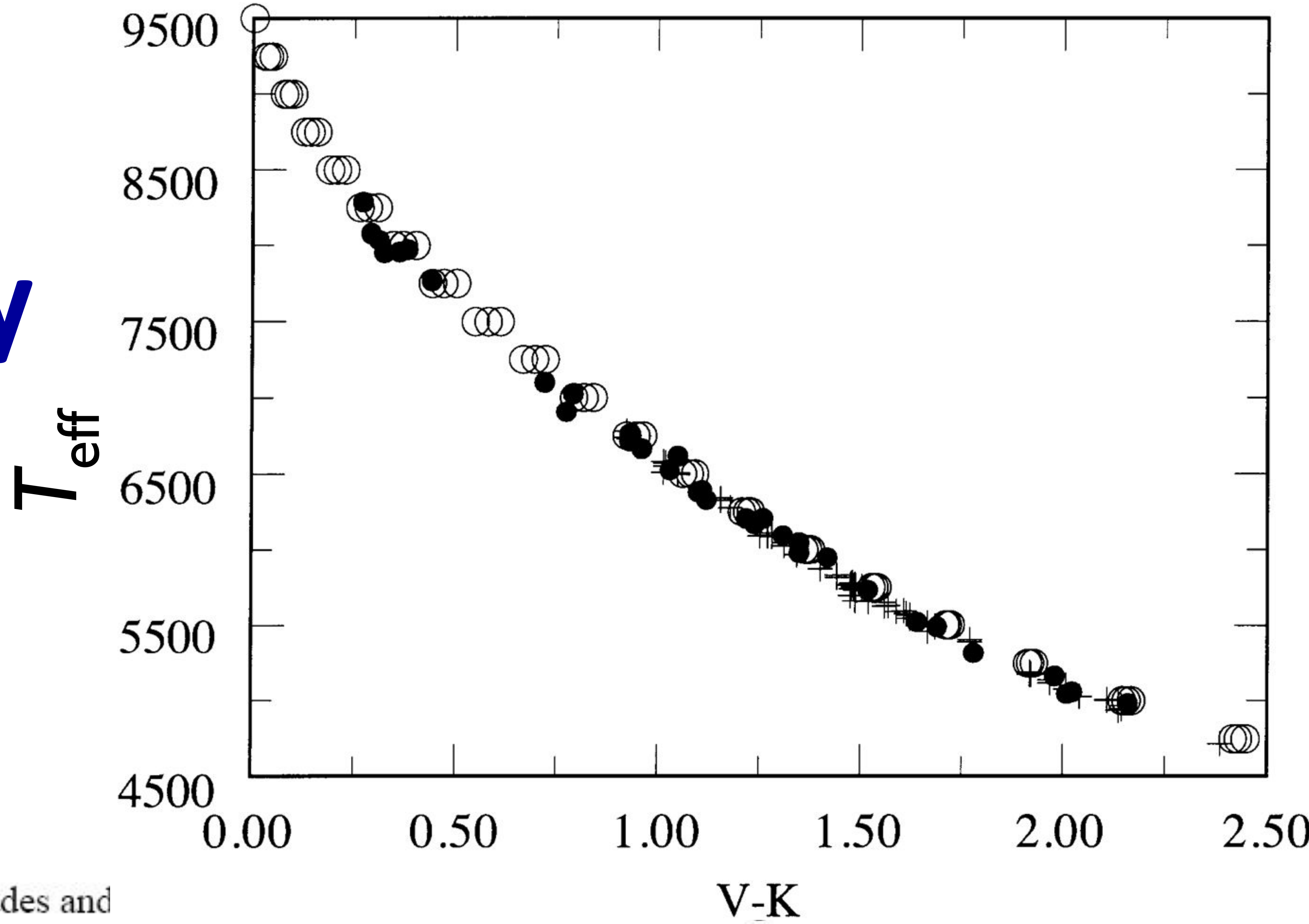

Table A3. Observed and model magnitudes and

	V	U-B	B-V	V-R	V-I	V-K	J-K	H-K	Ref
Sun	-26.76								Stebbins & Kron 1957
Sun_ref	-26.75	0.128	0.649	0.370	0.726	1.511	0.372	0.039	Colina et al. 1996
Analog		0.185	0.652	0.355	0.692	1.50	0.38	0.045	Cayrel de Strobel 1996; Table 6
Model	-26.77	0.135	0.679	0.367	0.725	1.524	0.373	0.041	SUN-OVER
Model	-26.77	0.145	0.667	0.361	0.715	1.524	0.376	0.032	SUN-NOVER

Broadband optical photometric systems

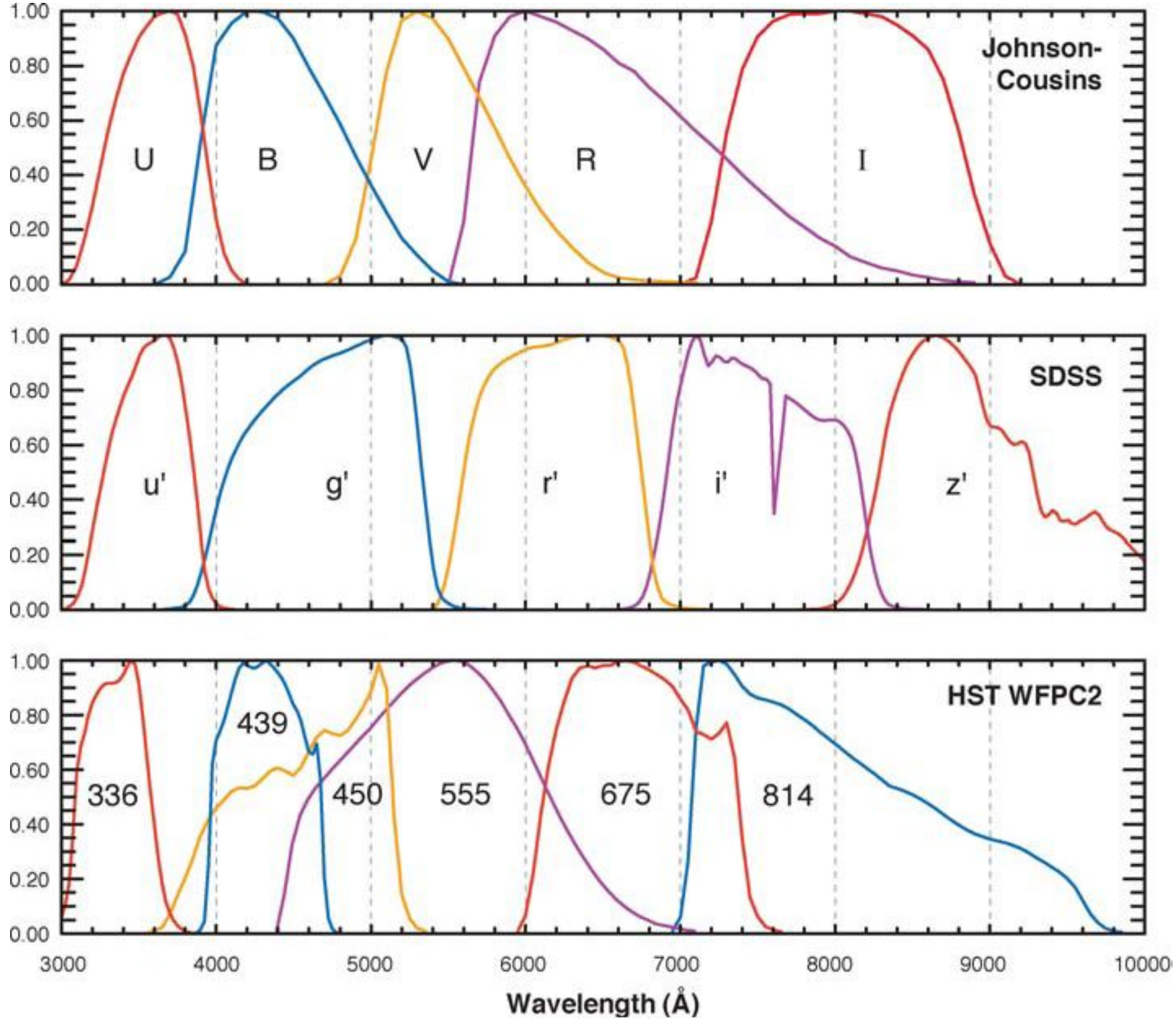

Bessell 2005, ARA&A

Optical Tycho and Infrared 2MASS systems

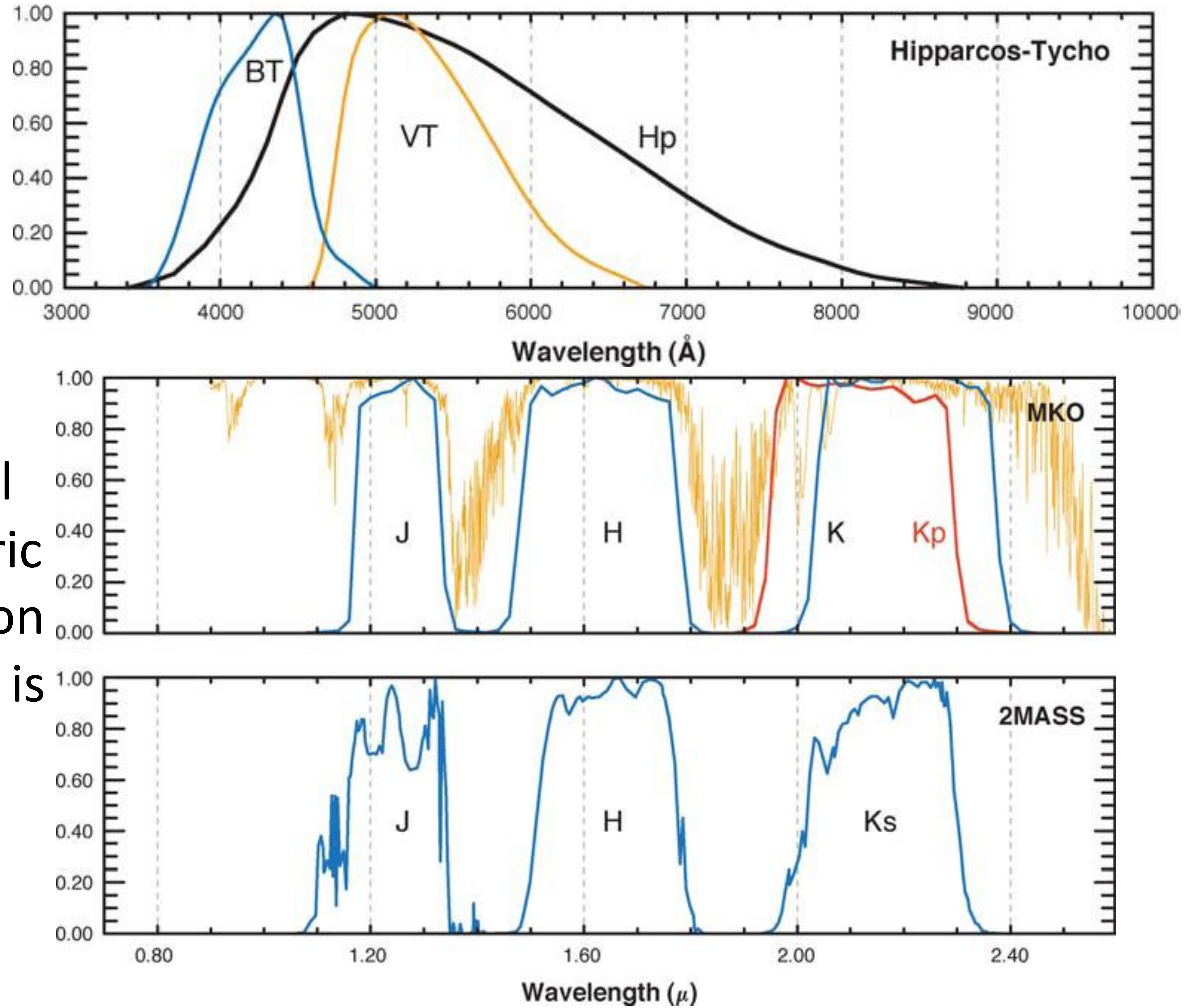

The terrestrial atmospheric transmission of a model is shown

Bessell 2005, ARA&A

A&A 512, A54 (2010)
DOI: 10.1051/0004-6361/200913204

Astronomy & Astrophysics

Improved calibrations: zero-point using solar twins

An absolutely calibrated $T_{\rm eff}$ scale from the infrared flux method

Dwarfs and subgiants*

L. Casagrande[1], I. Ramírez[1], J. Meléndez[2], M. B

hing, Germa

4150-762 Po
Observatory

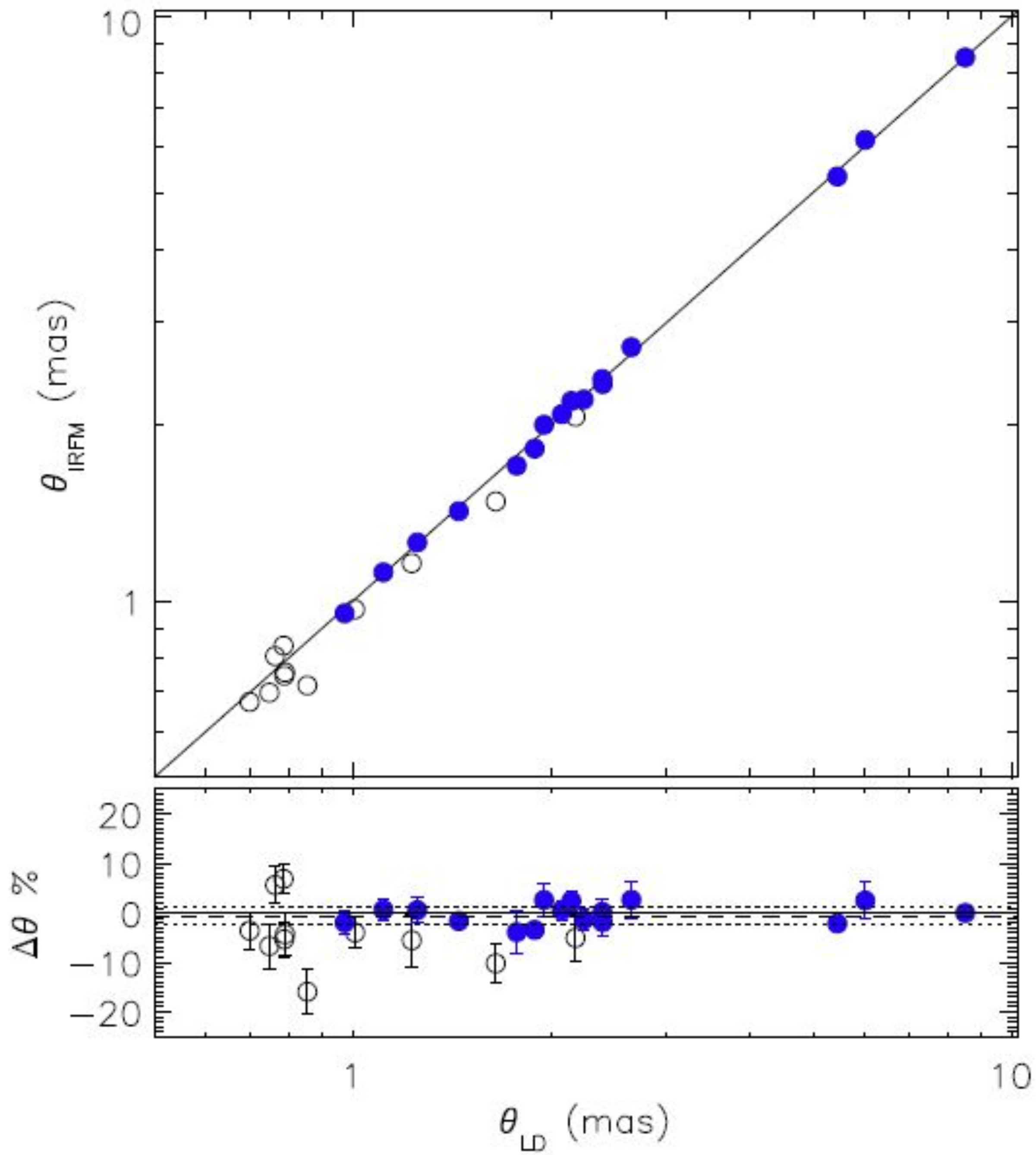

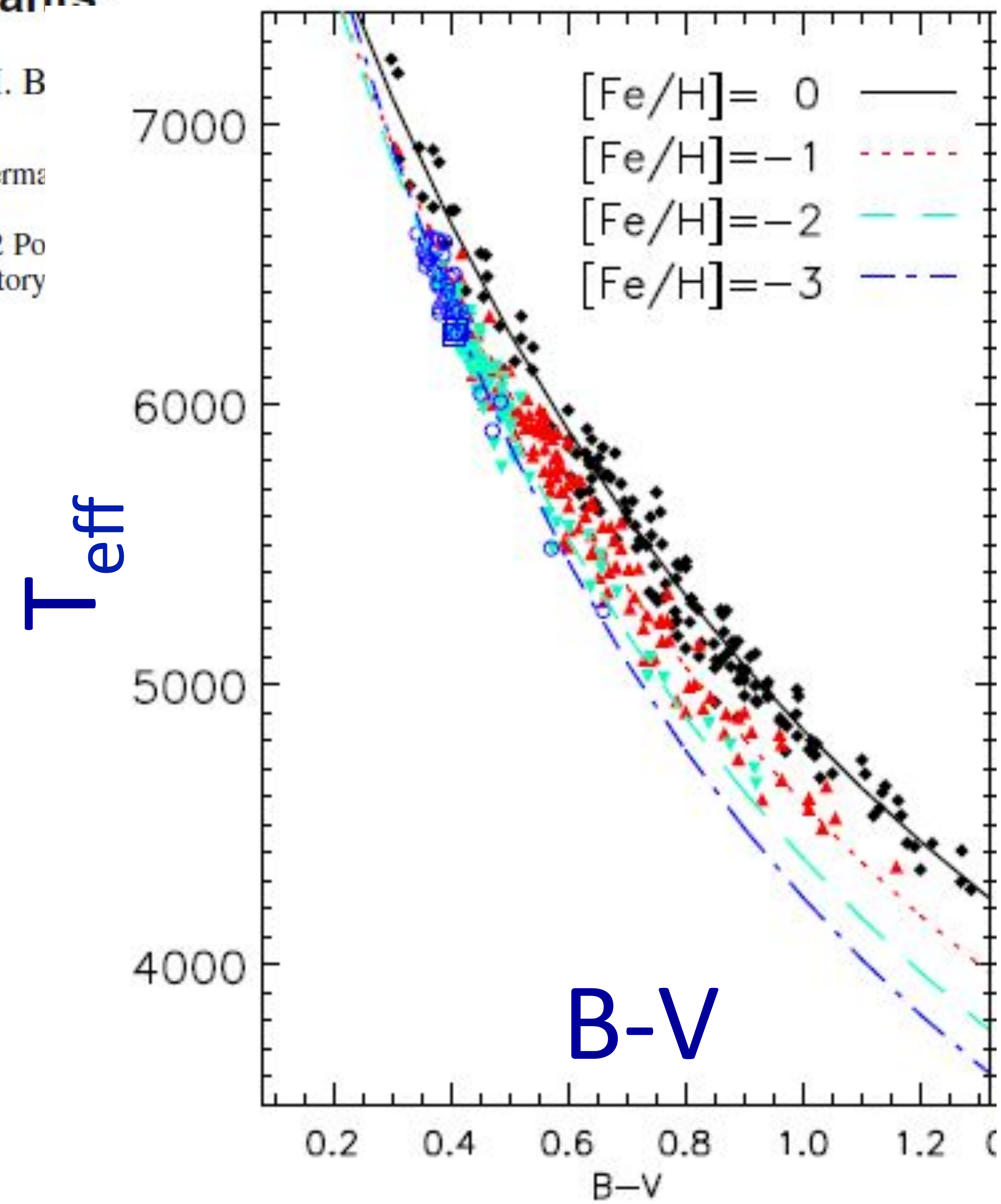

A&A 512, A54 (2010)
DOI: 10.1051/0004-6361/200913204

CaRaMBA

Astronomy & Astrophysics

An absolutely calibrated T_{eff} scale from the infrared flux method

Dwarfs and subgiants★

L. Casagrande[1], I. Ramírez[1], J. Meléndez[2], M. Bessell[3], and M. Asplund[1]

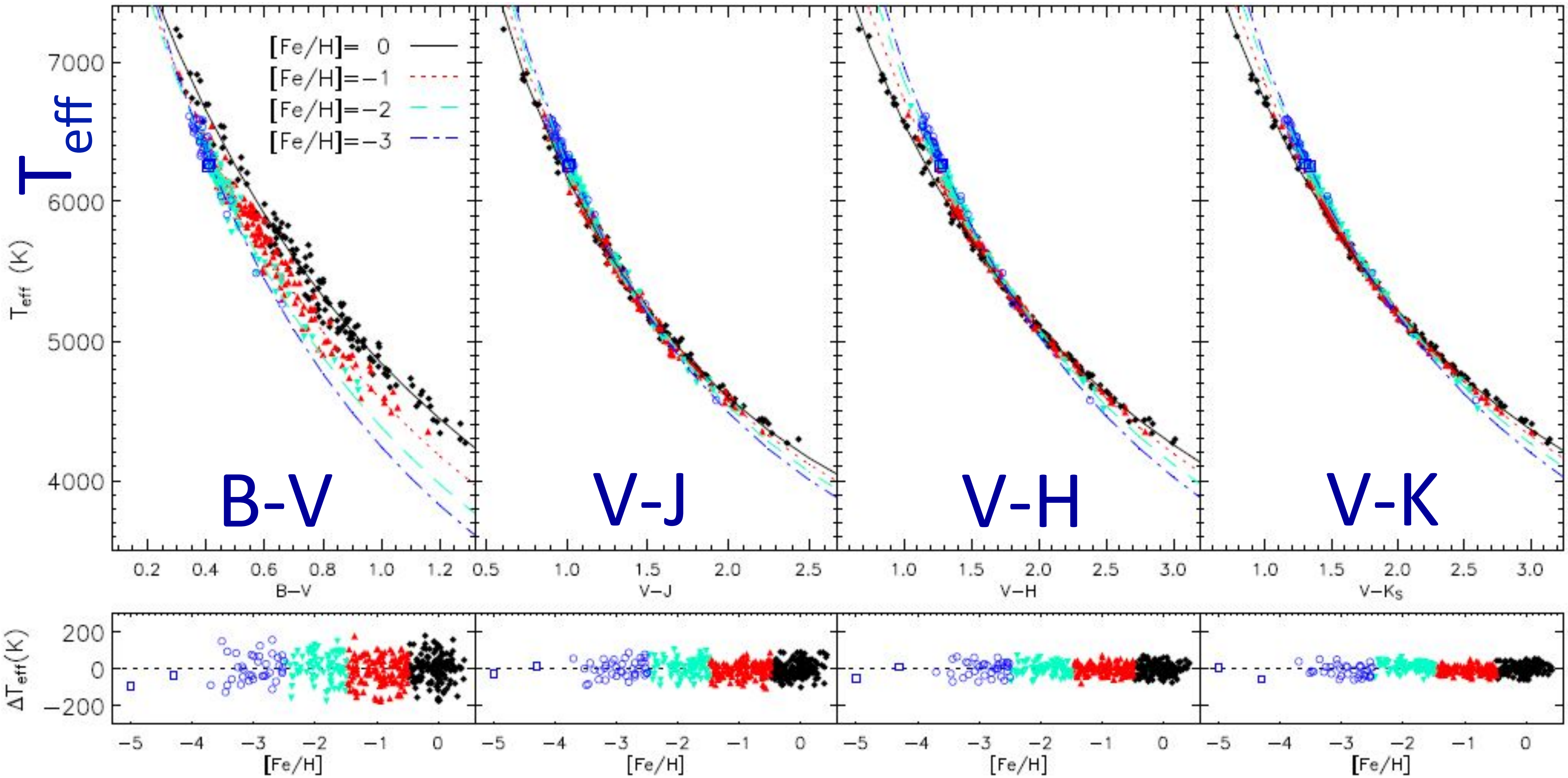

Fig. 14. Upper panels: empirical colour–temperature–metallicity calibrations in the metallicity bins $-0.5 < [Fe/H] \leq 0.5$ (filled diamonds), $-1.5 < [Fe/H] \leq -0.5$ (upward triangles), $-2.5 < [Fe/H] \leq -1.5$ (downward triangles) and $[Fe/H] \leq -2.5$ (open circles). Open squares are for the hyper metal-poor stars HE0233-0343 and HE1327-2326. Lower panels: residual of the fit as function of metallicity. For the two hyper-metal-poor stars, the residual is with respect to the fit at $[Fe/H] = -3.5$.

Effective temperature of M dwarfs

Mon. Not. R. Astron. Soc. 389, 585–607 (2008)

M dwarfs: effective temperatures, radii and metallicities

Luca Casagrande,[1★] Chris Flynn[1] and Michael Bessell[2]

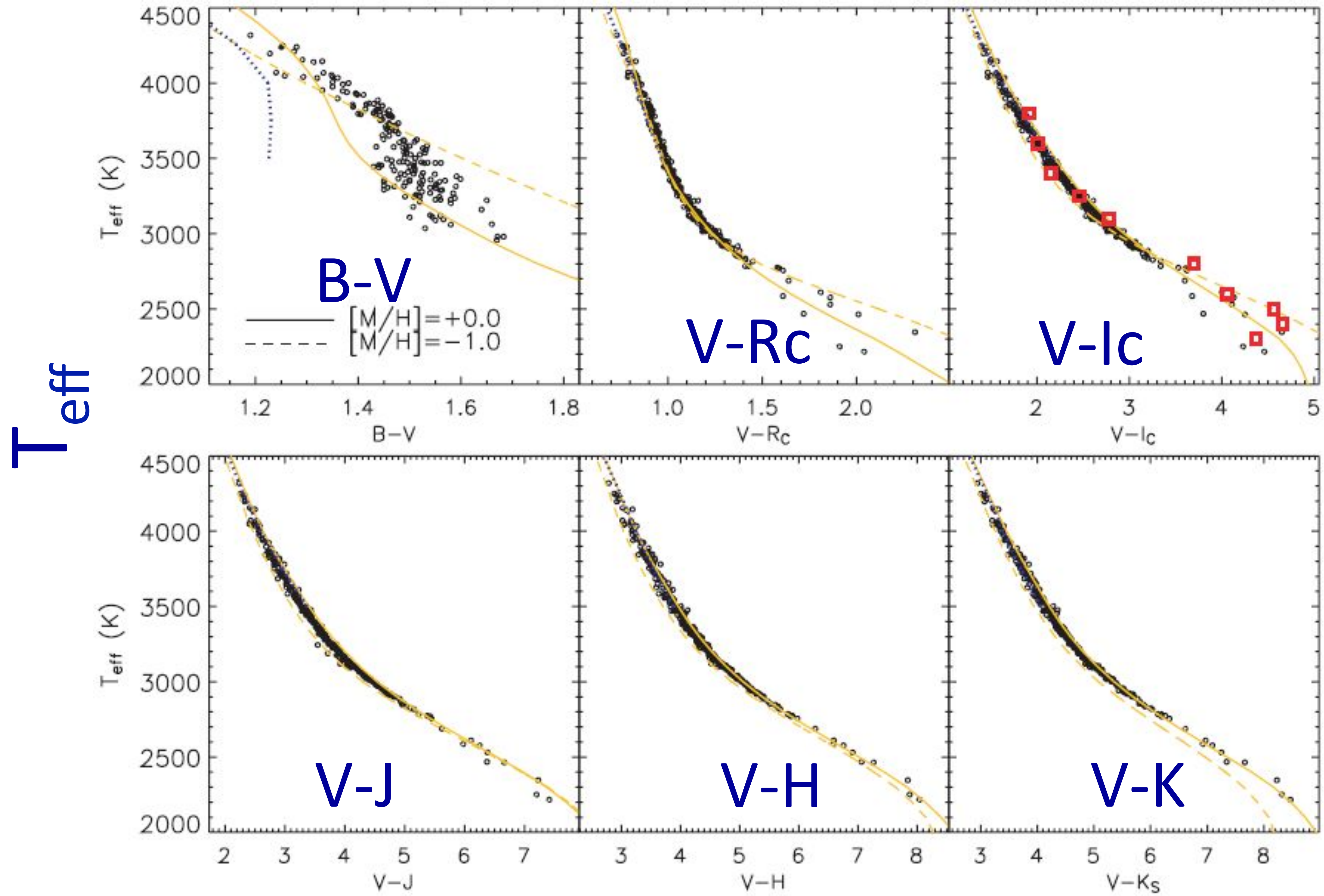

9. Colour–T_{eff} plots in different bands for our M dwarfs. Overplotted are the prediction from the Phoenix models (solid and dashed lines) for two nt metallicities which roughly bracket our sample of stars. Also shown for comparison the prediction from the Castelli & Kurucz (2003) models for ıetallicity (dotted line). Squares in the T_{eff} versus $V - I_C$ plot are from the temperature scale of Reid & Hawley (2005).

Intermediate band photometric systems

***uvby*-H_β**
Strömgren & Crawford 1956

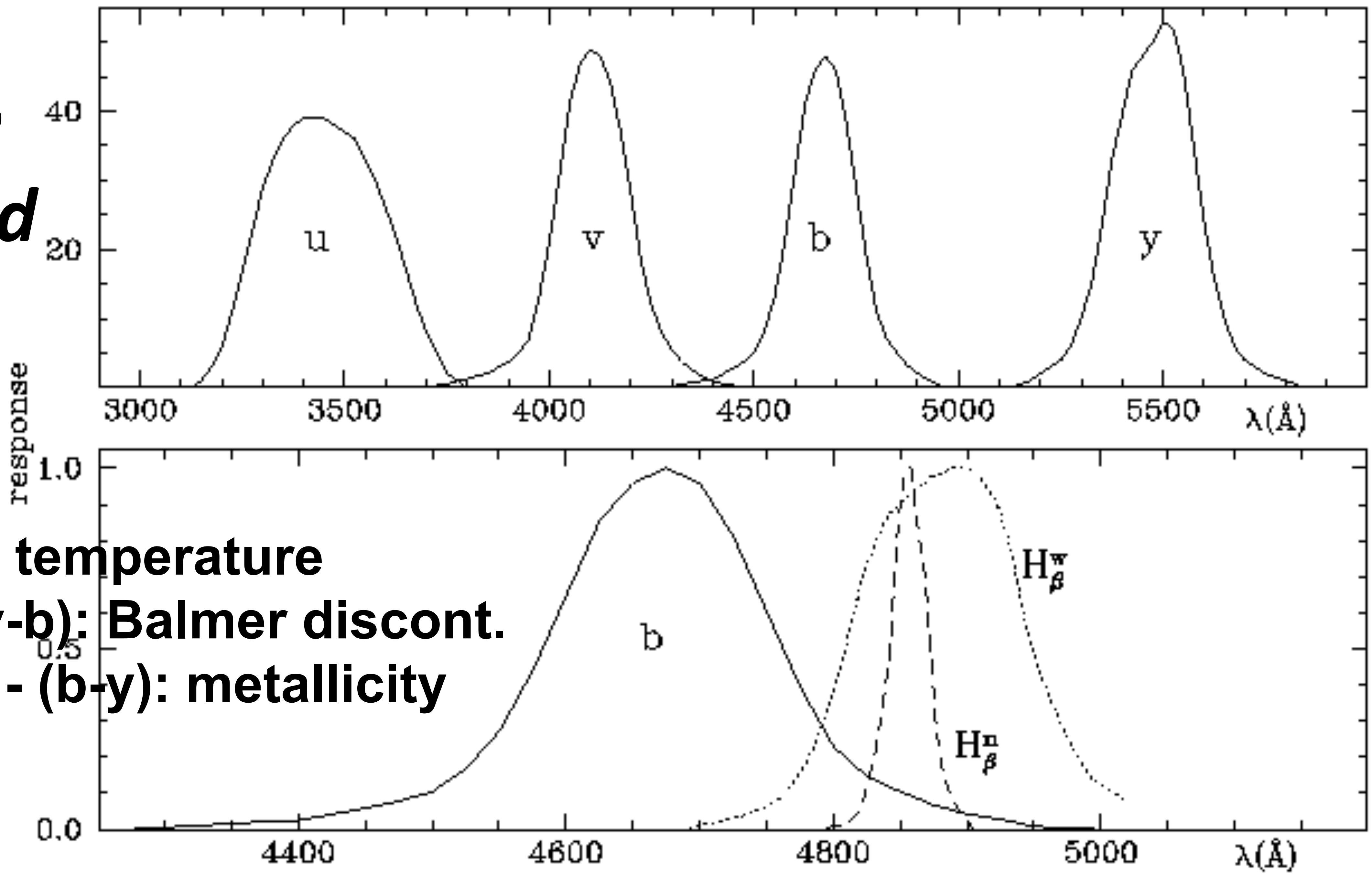

(b-y): temperature

c_1 = (u-v) - (v-b): Balmer discont.

m_1 = (v-b) - (b-y): metallicity

band	*u*	*v*	*b*	*y*	$H_{\beta n}$	$H_{\beta w}$
λ_{peak} (Å)	3500	4110	4670	5470	4859	4890
½Δλ (Å)	300	190	180	230	30	145

Önehag et al. 2009 A&A 498, 527

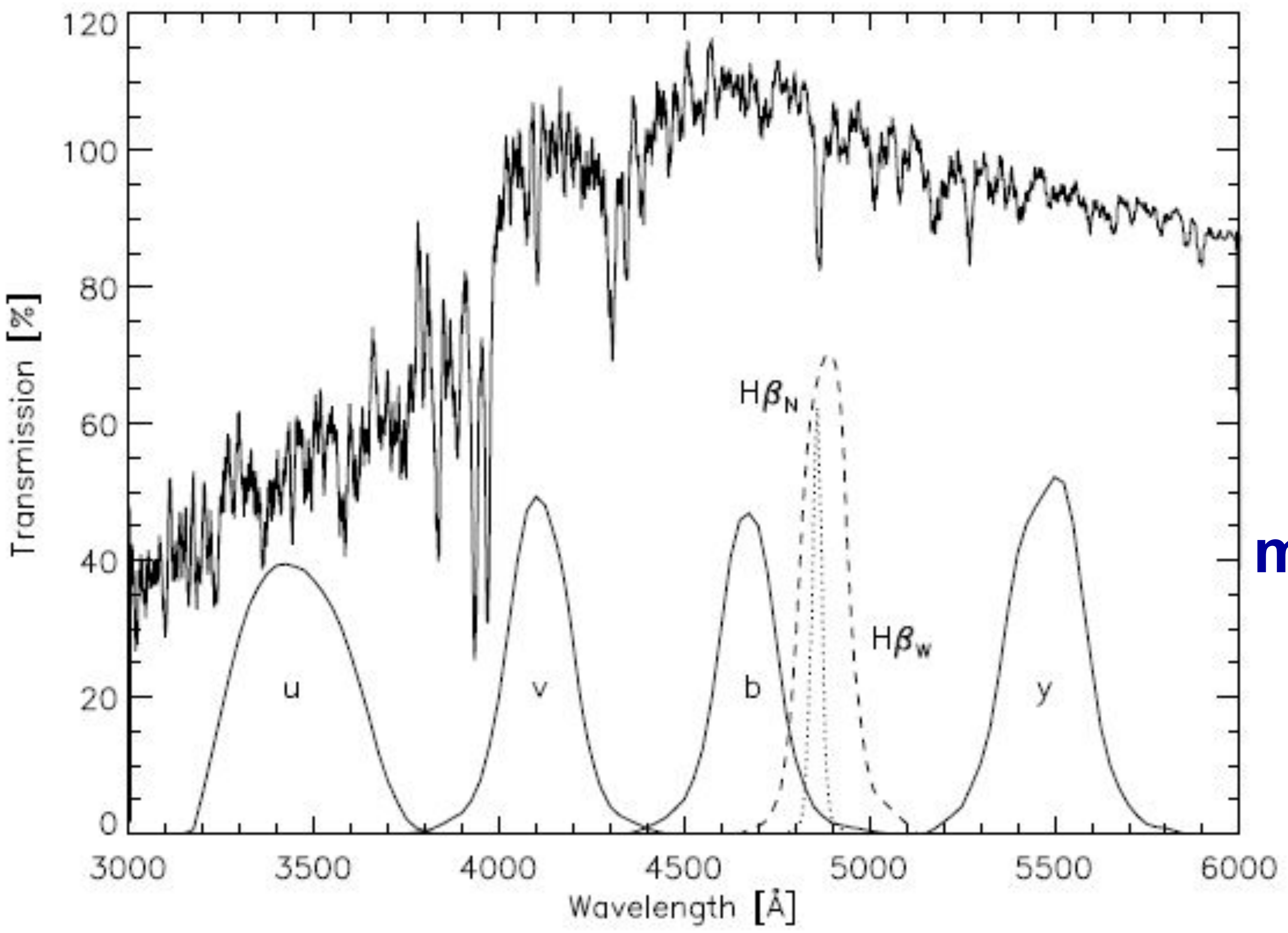

Fig. 1. The *uvby*–Hβ transmission functions of the standard systems plotted as a function of wavelength. As a comparison, the flux (per Ångström unit) of a model with $T_{eff} = 6000$ K, $\log g = 4.0$ and [Me/H] = 0.0 is plotted on an arbitrary flux scale.

(b-y): Temperature

m_1 = (v-b) - (b-y): metallicity

Relationship between spectral type and *b-y*

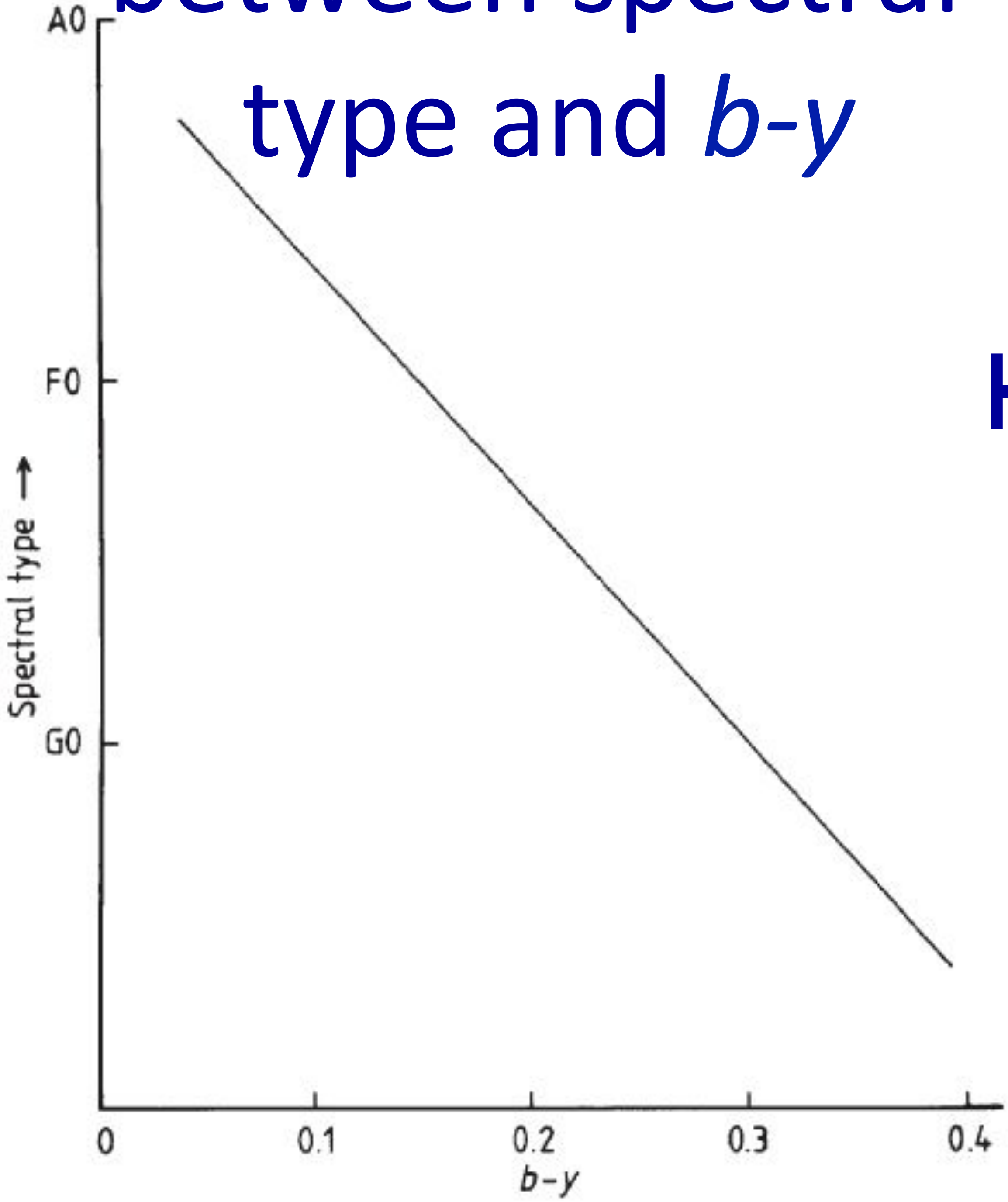

© Fig. 3.1.9, Kitchin

Relationship between T_{eff} and *b-y*

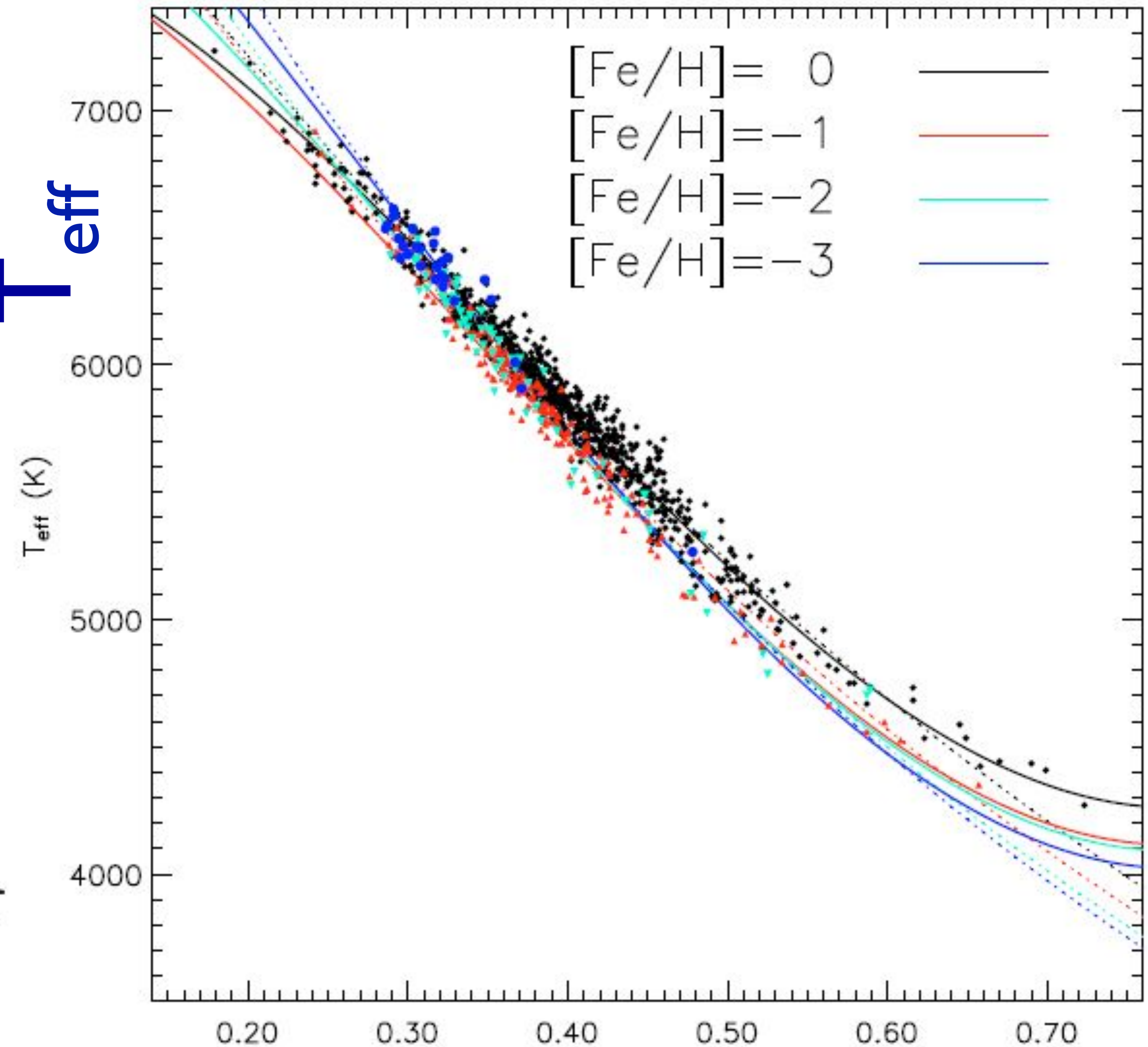

T_{eff}

b - y

A&A 512, A54 (2010)

L. Casagrande[1], I. Ramírez[1], J. Meléndez[2], M. Bessell[3], and M. Asplund[1]

ASTROPHYSICA NORVEGICA

VOL. IX NO. 31

1966, Ap. Norveiga 9, 333

ON THE CHEMICAL COMPOSITION AND KINEMATICS OF DISC HIGH-VELOCITY STARS OF THE MAIN SEQUENCE*

BY BENGT STRÖMGREN

Determining [Fe/H] using Δm_1

Hyades

$$\Delta m_1 = m_1(b - y) - m_1$$

indicates the difference in metal-hydrogen ratio of the star in question in comparison with the Hyades cluster members. A positive Δm_1 means that the metal content is low relative to that of the Hyades stars.

For the main-sequence F8–G2 stars investigated by Wallerstein [6] there is a close correlation between Δm_1 and the Fe/H ratio. Following Wallerstein we define

$$\left[\frac{\mathrm{Fe}}{\mathrm{H}}\right] = \log\left(\frac{\text{abundance of Fe}}{\text{abundance of H}}\right)_{\text{star}} - \log\left(\frac{\text{abundance of Fe}}{\text{abundance of H}}\right)_{\text{sun}}$$

It has been found (cf. [20]) that the Wallerstein [Fe/H] values for main-sequence stars around spectral class G0 are well represented by a linear relation

$$\left[\frac{\mathrm{Fe}}{\mathrm{H}}\right] = 0.3 - 12 \cdot \Delta m_1$$

and that [Fe/H] can be predicted from Δm_1 with an accuracy of about 0.1 (p. e.) for the category of stars in question.

H. Bond (1970, ApJS 22, 117): [Fe/H] = 0.16 - 13.6 Δm_1

$[Fe/H]_{uvby}$: Schuster & Nissen 1984

Schuster & Nissen 1984 (A&A 221, 65):

116 stars, $-2.6 < [Fe/H] < +0.4$

$0.37 < (b-y) < 0.59$, $0.03 < m_1 < 0.57$, $0.10 < c_1 < 0.47$

$$[Fe/H] = -2.0965 + 22.45\, m_1 - 53.8\, m_1^2 - 62.04\, m_1(b-y) + 145.5\, m_1^2(b-y) + [\,85.1\, m_1 - 13.8\, c_1 - 137.2 m_1^2\,]\, c_1$$ (s = 0.16 dex)

$[Fe/H]_{uvby}$: Ramírez & Meléndez 2005a

1. For $0.19 \le (b-y) < 0.35$, with $\sigma = 0.17$ dex,

$$[Fe/H] = -4.29 - 66.0 m_1 + 444.2 m_1(b-y) - 782.4 m_1(b-y)^2 + (0.966 - 37.8 m_1 - 1.707 c_1)\log\eta, \quad (6)$$

where $\eta = m_1 - [0.40 - 3.0(b-y) + 5.6(b-y)^2]$.

2. For $0.35 \le (b-y) < 0.50$, with $\sigma = 0.13$ dex,

$$[Fe/H] = -3.864 + 48.6 m_1 - 108.5 m_1^2 - 85.2 m_1(b-y) + 190.6 m_1^2(b-y) + [15.7 m_1 - 11.1 c_1 + 17.7(b-y)]c_1. \quad (7)$$

3. For $0.50 \le (b-y)_0 \le 0.80$, with $\sigma = 0.15$ dex,

$$[Fe/H] = -2.63 + 26.0 m_1 - 41.3 m_1^2 - 45.4 m_1(b-y) + 74.0 m_1^2(b-y) + 17.0 m_1 c_1. \quad (8)$$

Casagrande et al. (2011). New calibrations applied to GCS

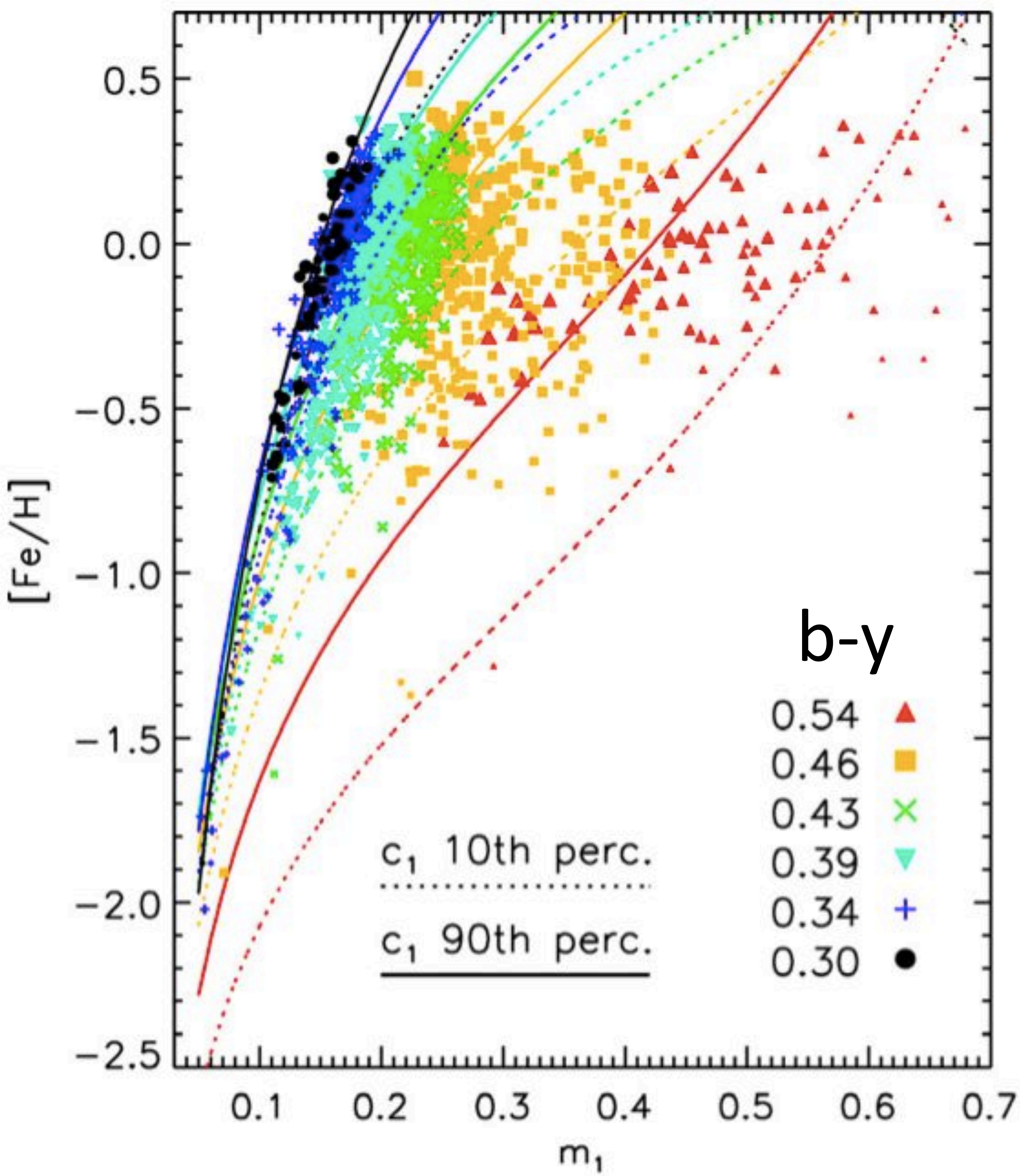

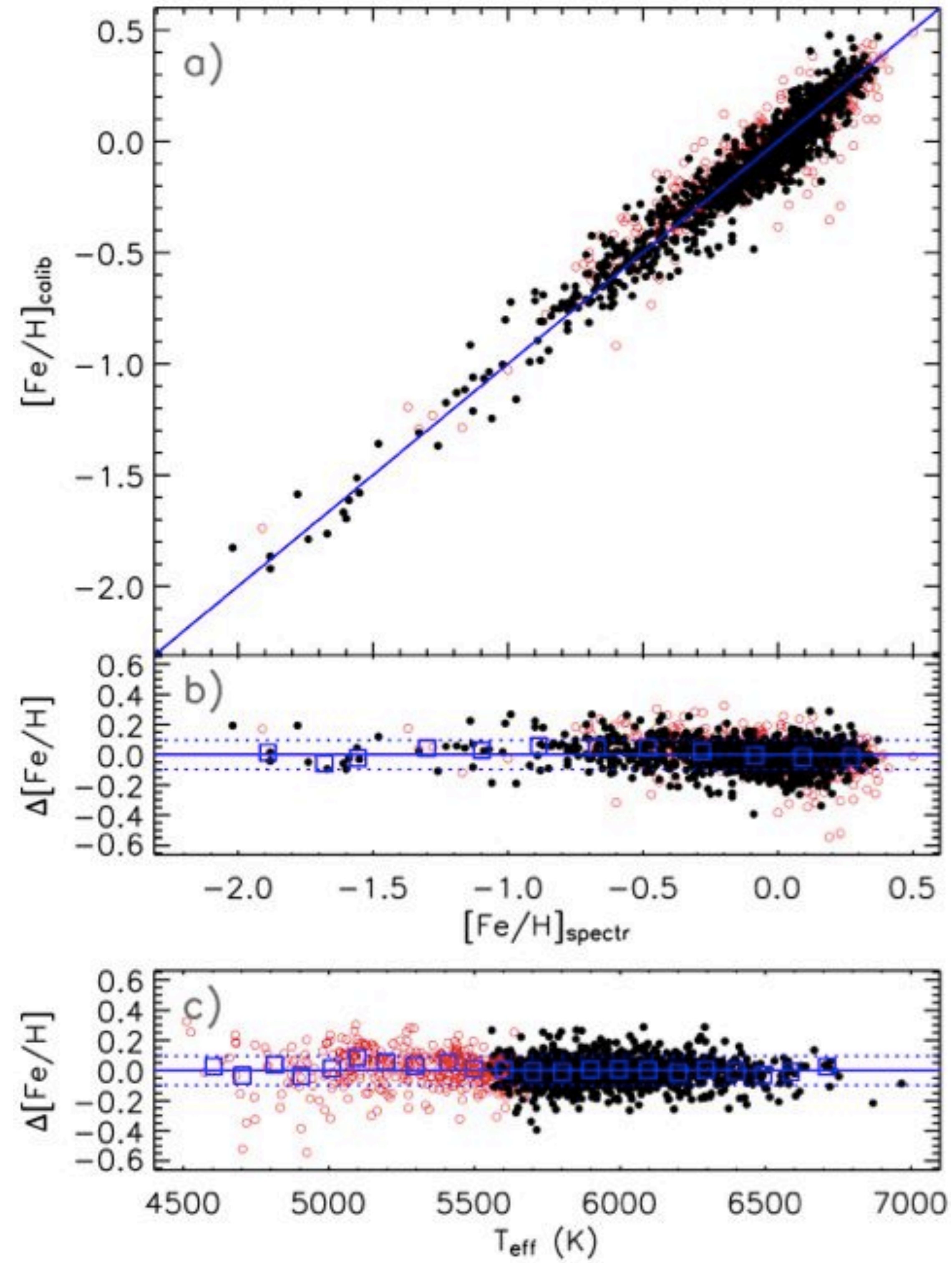

$$[\mathrm{Fe/H}] = 3.927\,\log(m_1) - 14.459\,m_1^3 - 5.394\,(b-y)\,\log(m_1)$$
$$+\,36.069\,(b-y)\,m_1^3 + 3.537\,c_1\,\log(m_1)$$
$$-\,3.500\,m_1^3\,c_1 + 11.034\,(b-y) - 22.780\,(b-y)^2$$
$$+\,10.684\,c_1 - 6.759\,c_1^2 - 1.548, \quad (2)$$

Casagrande et al. (2011): calibrating also [α/Fe]!

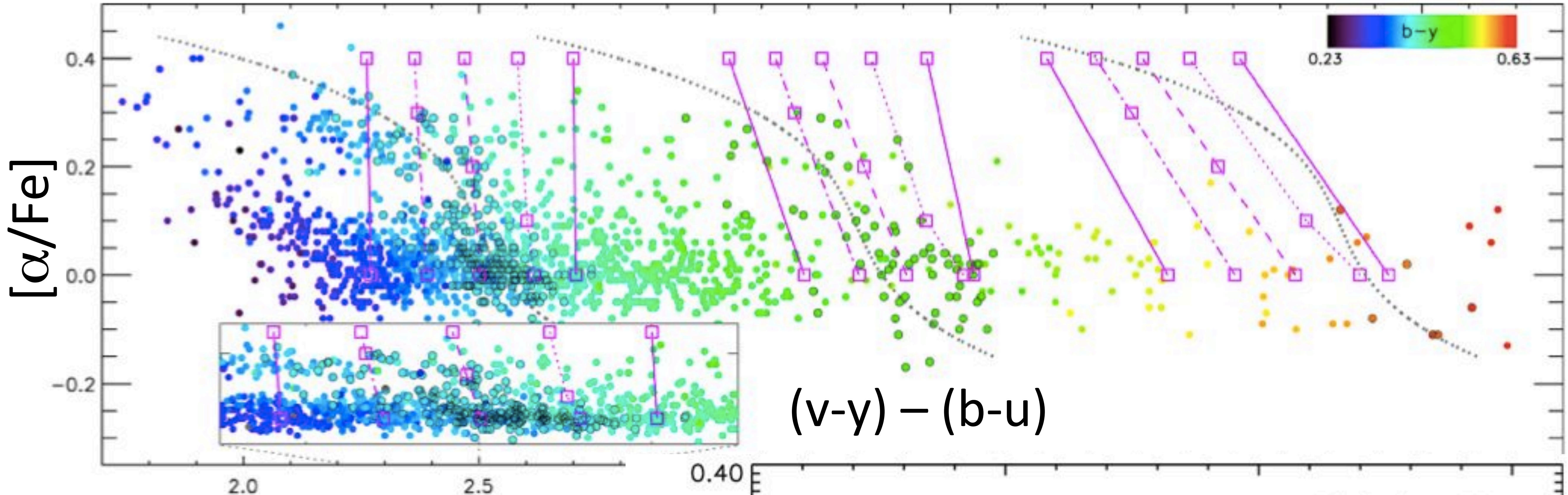

Fig. 9. [α/Fe] versus $(v-y)-(b-u)$ for our 1498 calibra
as shown in the top right box. Squares are synthetic colo
library) for selected values of $(b-y)$ = 0.4, 0.5, 0.6 (from l
−0.25 dex with [α/Fe] = 0:0.1:0.4 dex (dotted lines), [Fe
[α/Fe] = 0:0.3:0.4 dex (dot-dashed lines), [Fe/H] = −
selected $(b-y)$ interval are shown with open circles to h
a zoom of the $(b-y)$ = 0.4 data set for $2.2 \le (v-y)-($

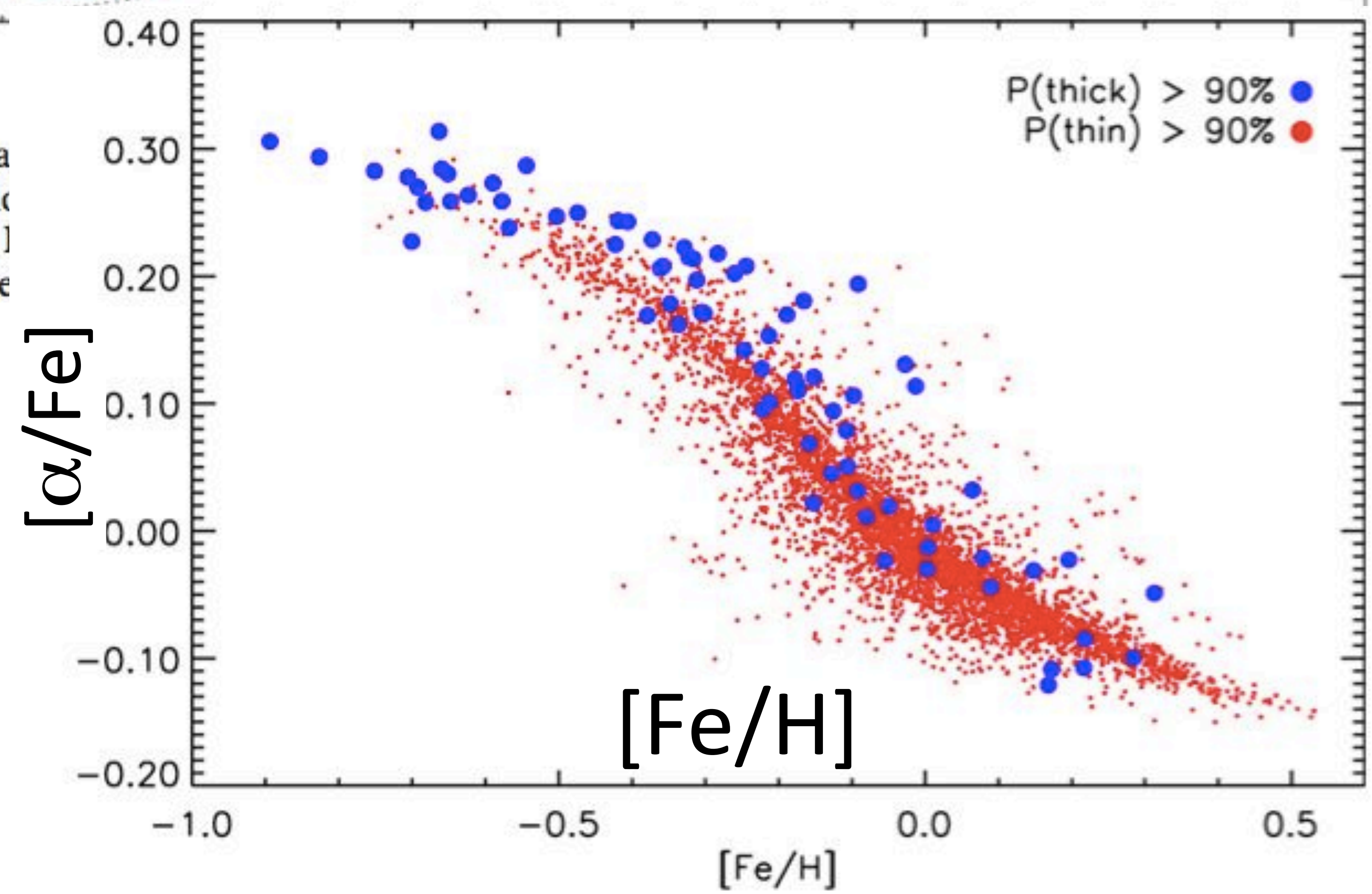

Interstellar reddening and extinction

Interstellar extinction A_X

$$A_X \equiv m_X - m_{X0} \Rightarrow m_{X0} = m_X - A_X$$

- A_X: extinction
- m_X: observed magnitude
- m_{X0}: intrinsic magnitude (what would be observed without interstelar dust)

Color excess E(X-Y)

$$E(X\text{-}Y) \equiv (m_X - m_Y) - (m_{X0} - m_{Y0})$$

- $m_X - m_Y$: observed color
- $m_{X0} - m_{X0}$: intrinsic color

$$E(X\text{-}Y) \equiv (m_X - m_{X0}) - (m_Y - m_{Y0})$$

$$E(X\text{-}Y) \equiv A_X - A_Y$$

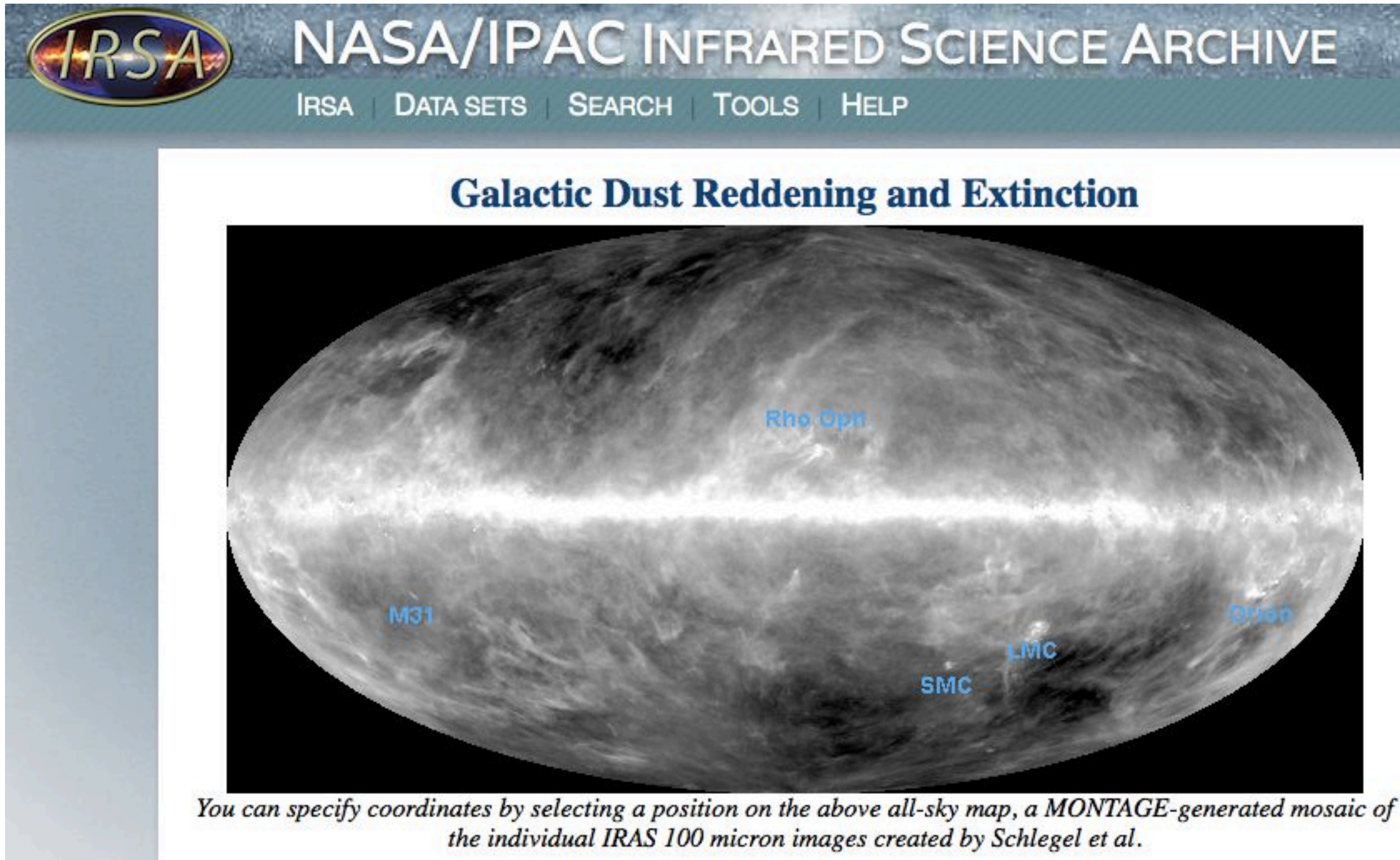

Surface gravity

$$g = \frac{GM}{R^2}$$

$$\log\left(\frac{g}{g_\odot}\right) = \log\left(\frac{M}{M_\odot}\right) + 4\log\left(\frac{T_{eff}}{T_{eff,\odot}}\right) + \log\left(\frac{L_\odot}{L}\right)$$

Trigonometric surface gravity

$$\log\left(\frac{g}{g_\odot}\right) = \log\left(\frac{M}{M_\odot}\right) + 4\log\left(\frac{T_{eff}}{T_\odot}\right) + 0.4V + 0.4BC + 2\log\pi + 0.1056$$

MSc dissertation (USP), Jhon Yana Galarza

Trigonometric surface gravity

$$\log\left(\frac{g}{g_{\odot}}\right) = \log\left(\frac{M}{M_{\odot}}\right) + 4\log\left(\frac{T_{eff}}{T_{\odot}}\right) + 0.4V + 0.4BC + 2\log\pi + 0.1056$$

Parallax (π)

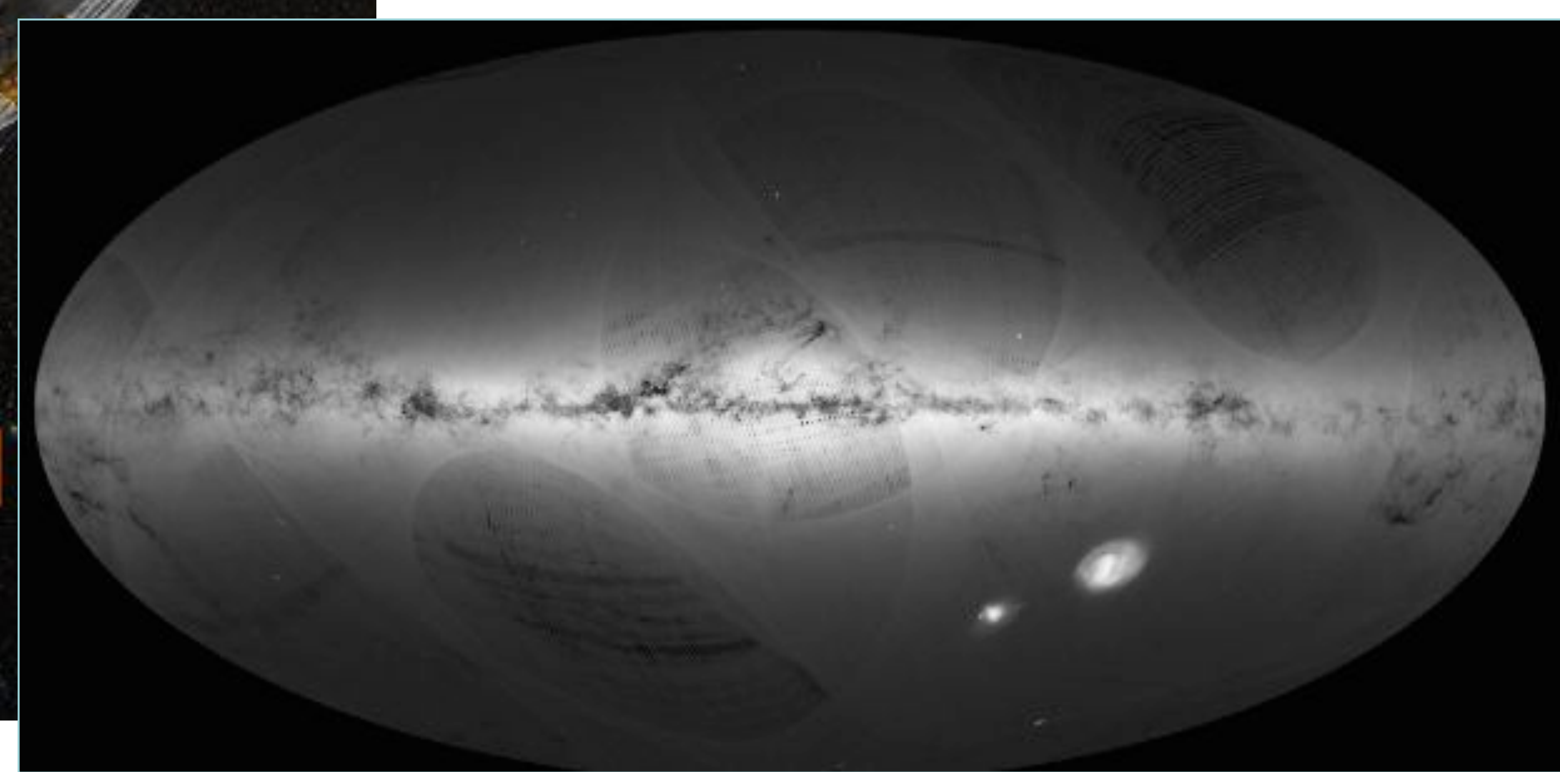

Determining Stellar Parameters by Spectroscopic Equilibrium

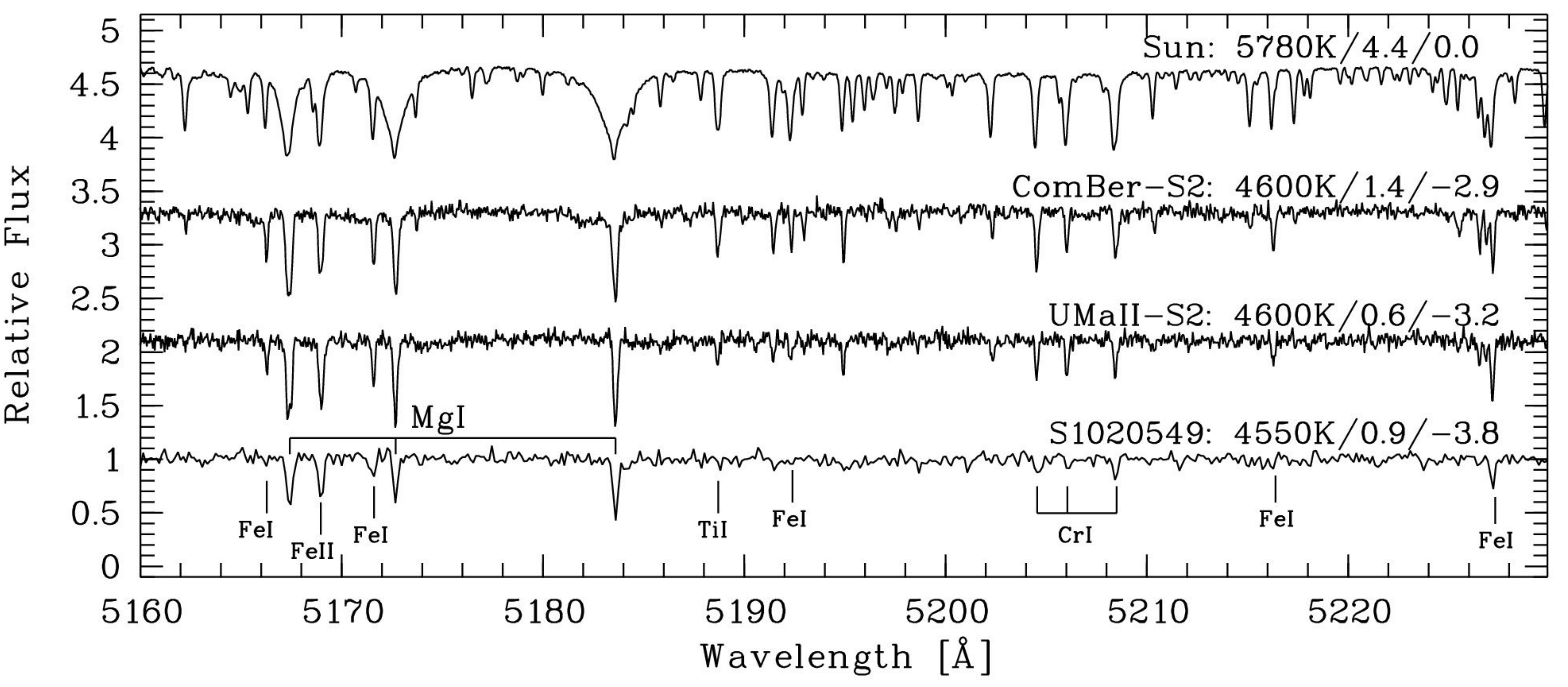

Energy levels of the H atom

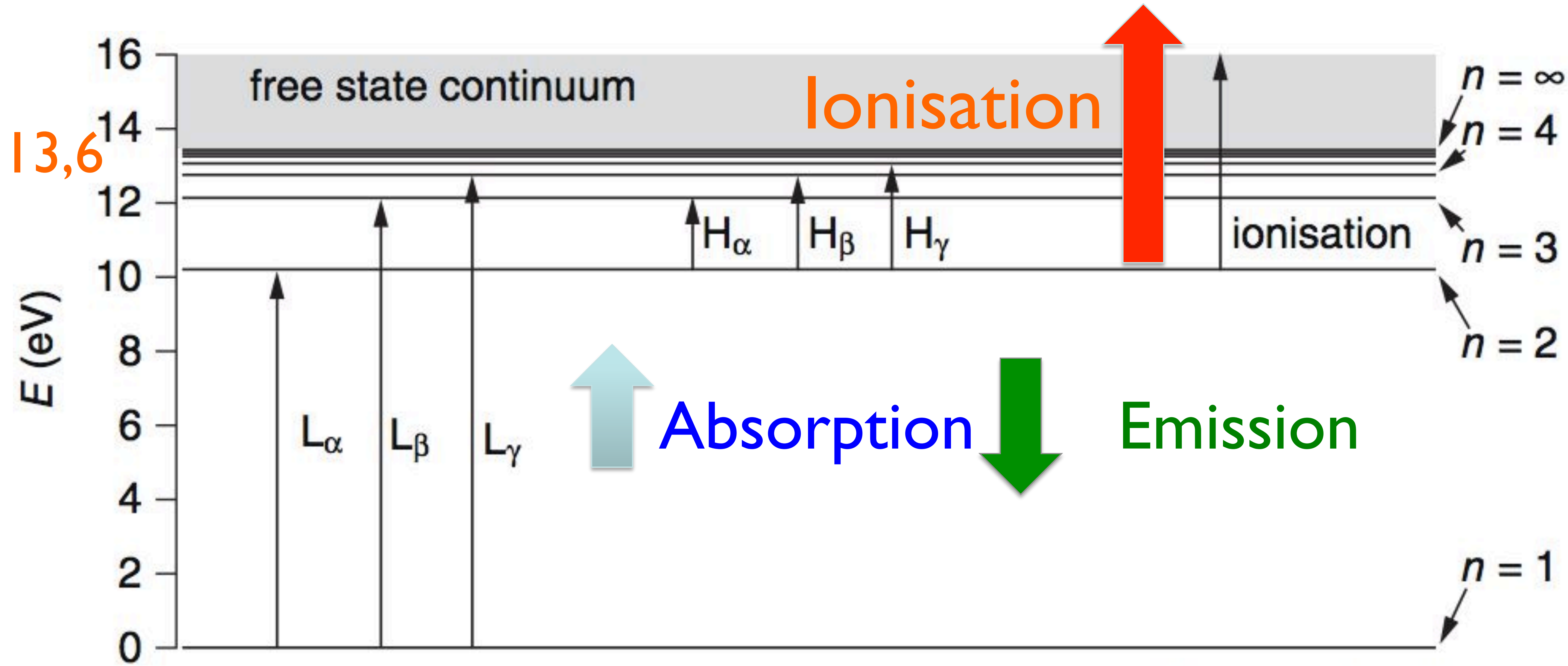

Energy levels of hydrogen in eV: $$E_n = 13.6\left[1 - \frac{1}{n^2}\right]$$

F. LeBlanc, Stellar Astrophysics

Energy level diagram

(*term* or *Grotrian diagram*)

for Na I

What is the chance of populating a given level?

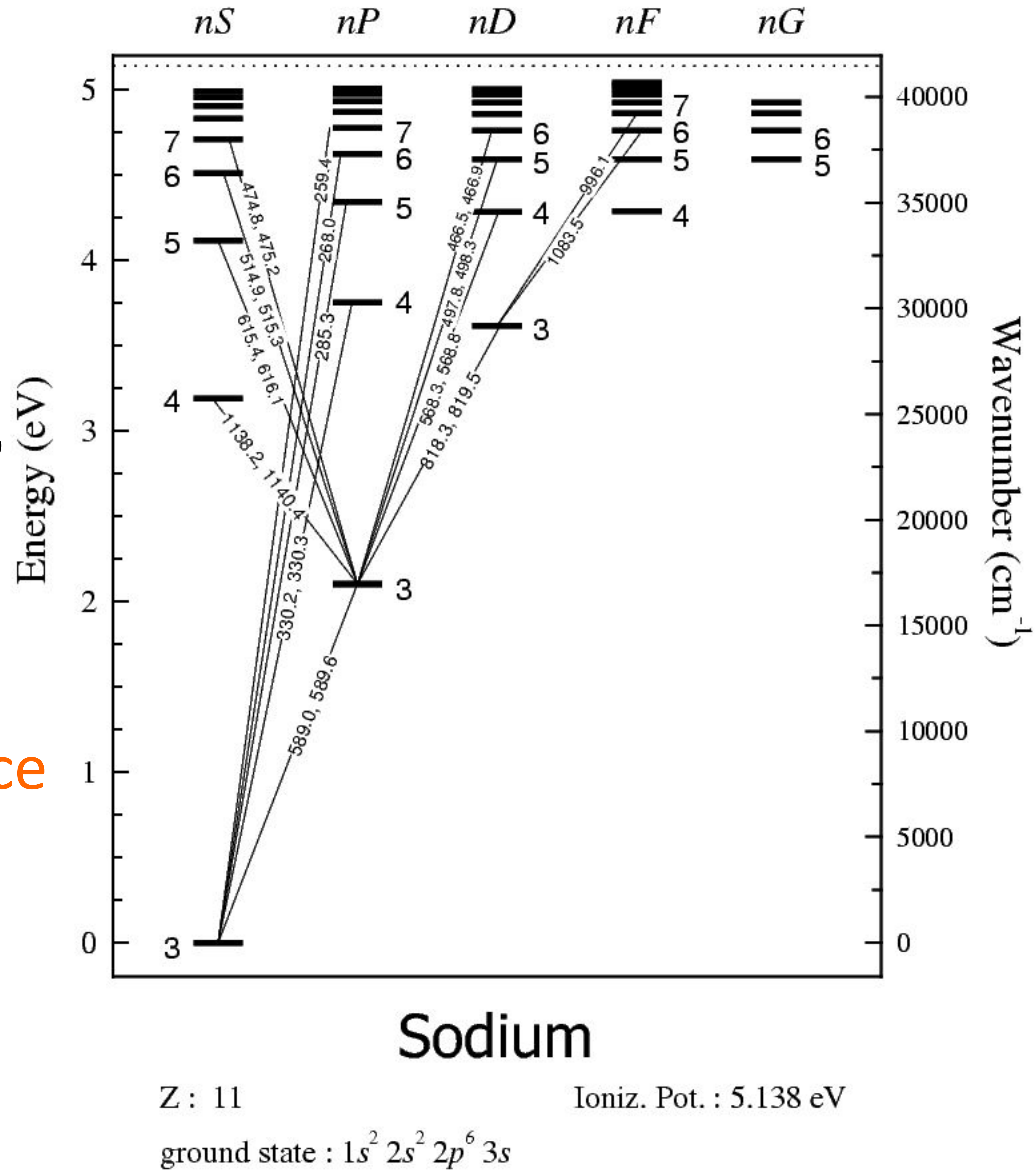

http://128.104.164.100/data/e_sodium.gif

Population of level *n* (Boltzmann Equation)

$$\frac{N_n}{N_m} = \frac{g_n}{g_m} e^{-\Delta\chi/kT}$$

Boltzmann population of a level *n*:

$$\frac{N_n}{N} = \frac{g_n e^{-\chi_n/kT}}{g_1 + g_2 e^{-\chi_2/kT} + g_3 e^{-\chi_3/kT} + \cdots}$$

$$= \frac{g_n}{u(T)} e^{-\chi_n/kT}$$

$$u(T) = \sum g_i e^{-\chi_i/kT}$$

u(T) is the partition function

Population of level *n* (Boltzmann Equation)

$$\frac{N_n}{N} = \frac{g_n}{u(T)} e^{-\chi_n/kT}$$

$$\frac{N_n}{N} = \frac{g_n}{u(T)} 10^{-\theta \chi_n}$$

The excitation potential χ_n in eV

$\theta = 5040/T$

5040 = (log e) / k ; k = 8.61733 x 10^{-5} eV K^{-1}

Ionisation: Notation

Neutral hydrogen: H, H^0 or H I

Ionized hydrogen: H^+ or H II

Neutral iron: Fe, Fe^0 or Fe I

Ionized iron: Fe^+ or Fe II

Iron three times ionized: Fe^{3+}, Fe IV

Populations:

- N_n: *n* level
- N_I: neutral; N_{II}: ionized, N_{III}: 2 times ionized
- N_n^{II}: excited level *n* in ionized atom

Ionization energies

Table D.1. *Atomic weights and ionization potentials.*

No.	Element	Symbol	Weight	I_1	I_2	I_3
1	Hydrogen	H	1.008	13.598	–	–
2	Helium	He	4.003	24.587	54.418	–
3	Lithium	Li	6.941	5.392	75.640	122.454
4	Beryllium	Be	9.012	9.323	18.211	153.897
5	Boron	B	10.811	8.298	25.155	37.931
6	Carbon	C	12.011	11.260	24.383	47.888
7	Nitrogen	N	14.007	14.543	29.601	47.449
8	Oxygen	O	15.994	13.618	35.117	54.936
9	Fluorine	F	18.998	17.423	34.971	62.708
10	Neon	Ne	20.179	21.565	40.963	63.45
11	Sodium	Na	22.990	5.139	47.286	71.620
12	Magnesium	Mg	24.305	7.646	15.035	80.144
13	Aluminum	Al	26.982	5.986	18.829	28.448
14	Silicon	Si	28.086	8.152	16.346	33.493
15	Phosphorus	P	30.974	10.487	19.769	30.203
16	Sulfur	S	32.06	10.360	23.338	34.79
17	Chlorine	Cl	35.45	12.968	23.814	39.61
18	Argon	Ar	39.95	15.760	27.63	40.74
19	Potassium	K	39.10	4.341	31.63	45.806
20	Calcium	Ca	40.08	6.113	11.872	50.913

D. Gray, Stellar Photospheres, 3rd Ed.

Ionization stages

The Saha equation

$$\frac{N_{II}}{N_I} P_e = \frac{(2\pi m_e)^{2/3} (kT)^{5/2}}{h^3} \frac{2u_1(T)}{u_0(T)} e^{-I/kT}$$

N_{II}/N_I : ratio of ions to neutrals
P_e : electron pressure
I : ionization potential
T : temperature
u_1/u_0 : ratio of ionic to neutral partition functions
k : Boltzmann constant, h: Planck constant, m_e = mass e-

The amount of ionization depends inversely on P_e

Spectroscopic Parameters

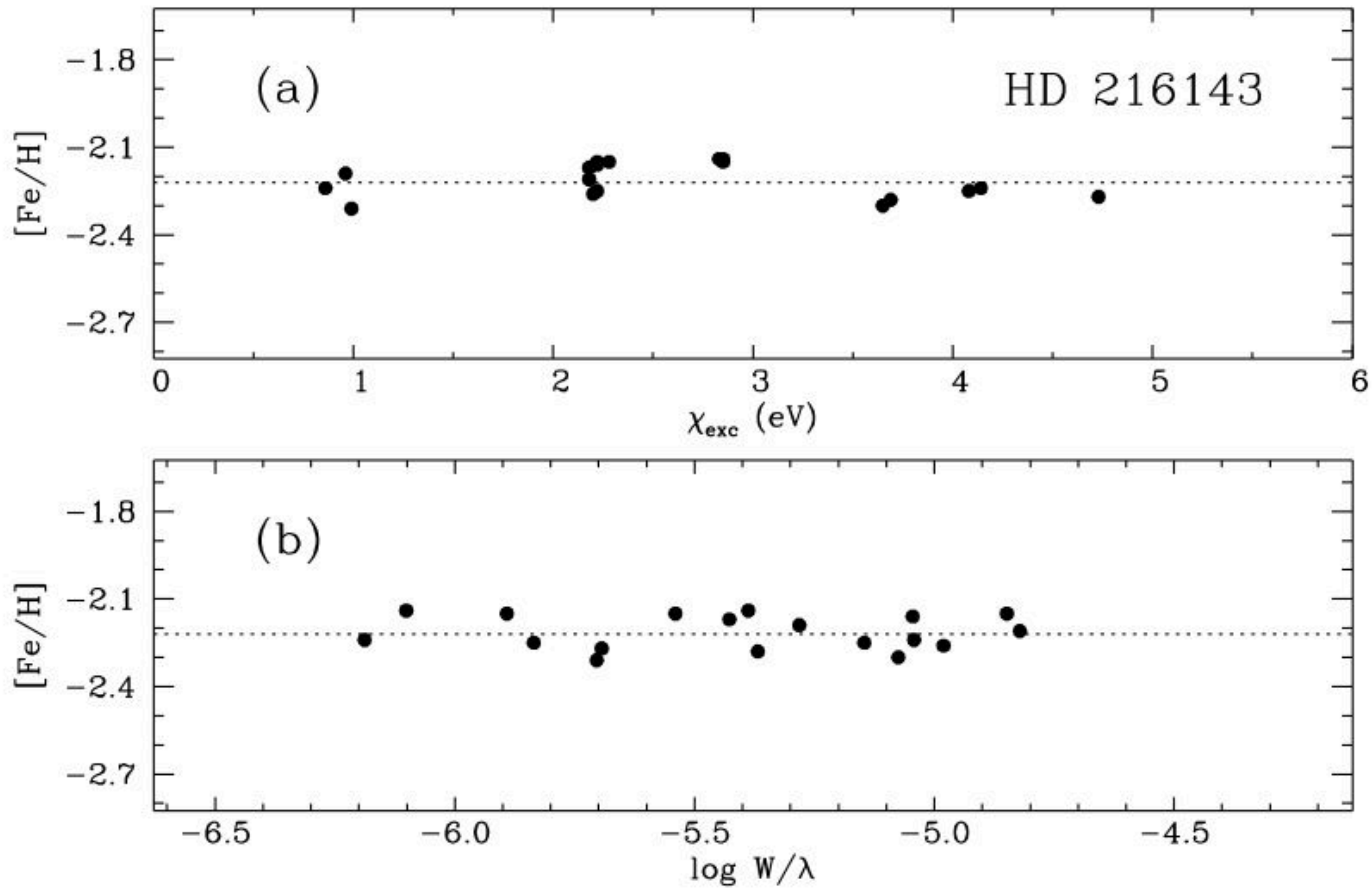

FIG. 2.—[Fe/H] vs. (*a*) excitation potential χ_{exc} and (*b*) reduced equivalent width W/λ for the spectroscopic parameters of HD 216143. There is no significant trend with χ_{exc} or log W/λ.

Meléndez et al. 2001

Ramírez, Meléndez, Cornejo et al. 2011, ApJ, 740, 76

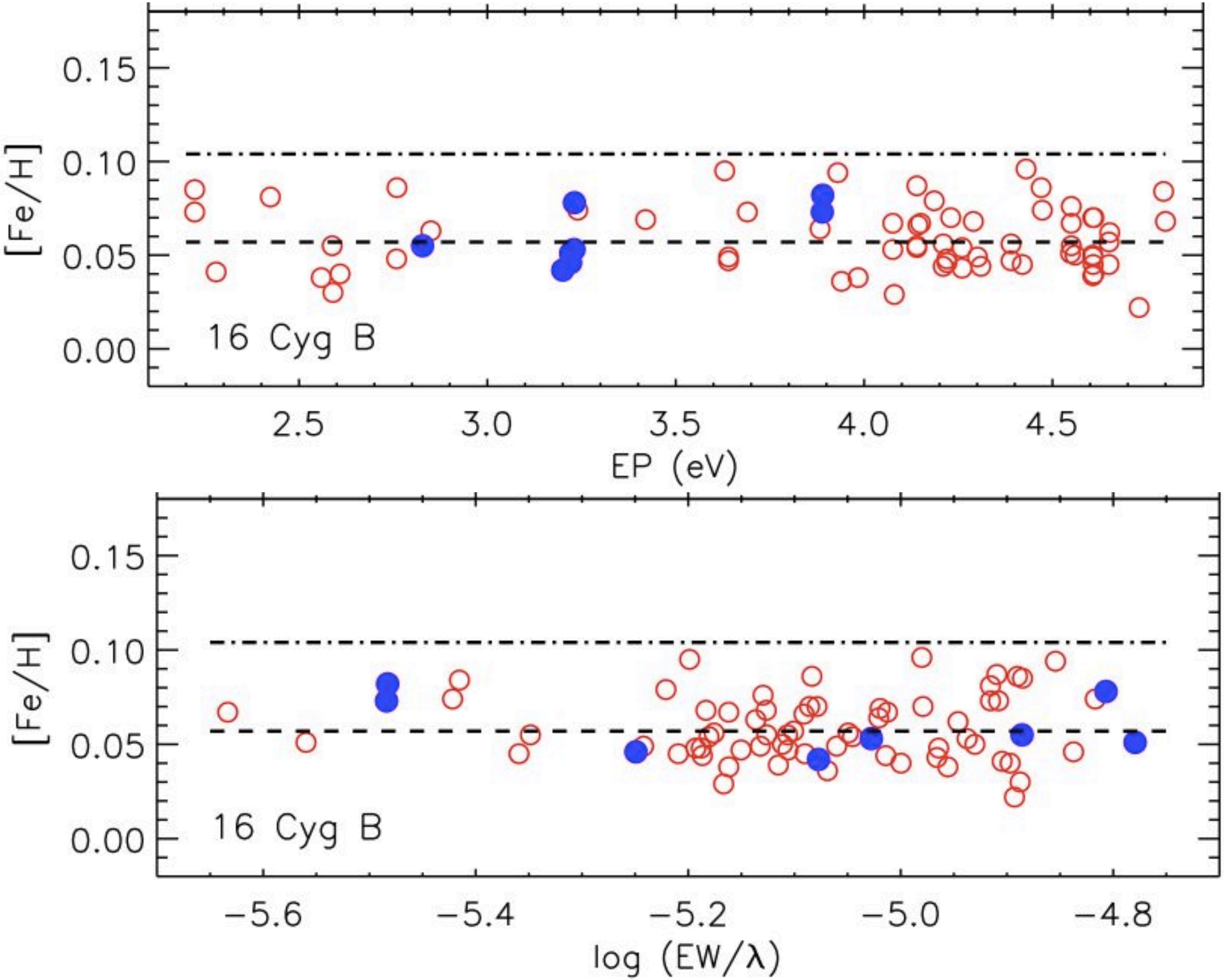

Spectroscopic Parameters

Equilíbrio de excitação

$$\frac{d(\delta A_{Fe,i})}{d\chi_{exc}} = 0$$

Teff = 5837 K

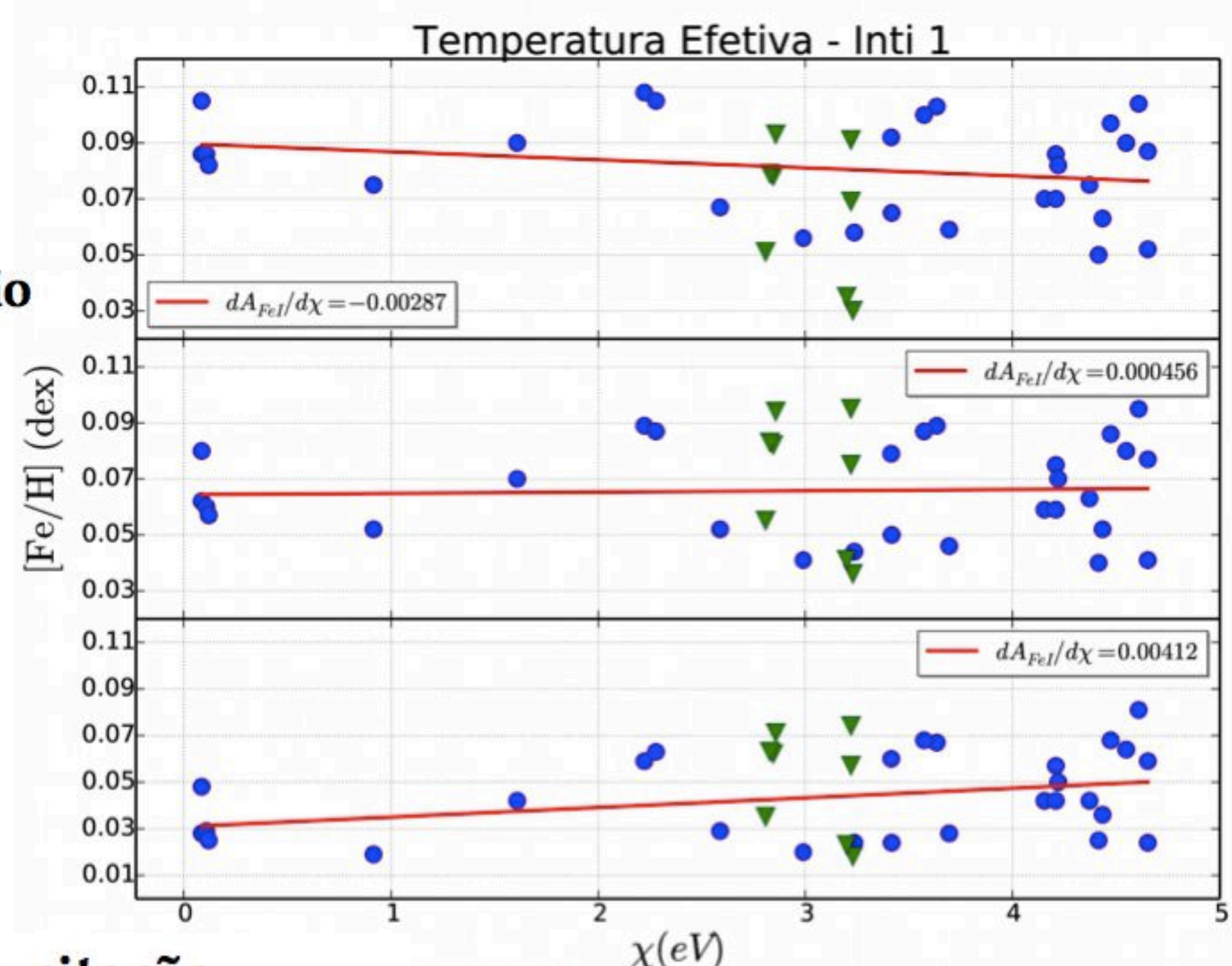

Equilíbrio de excitação

kms^{-1}

$$< \delta A_{FeII,i} > - < \delta A_{FeI,i} > = 0$$

Slide: Jhon Yana Galarza

Log *g* from strong lines: Na I D

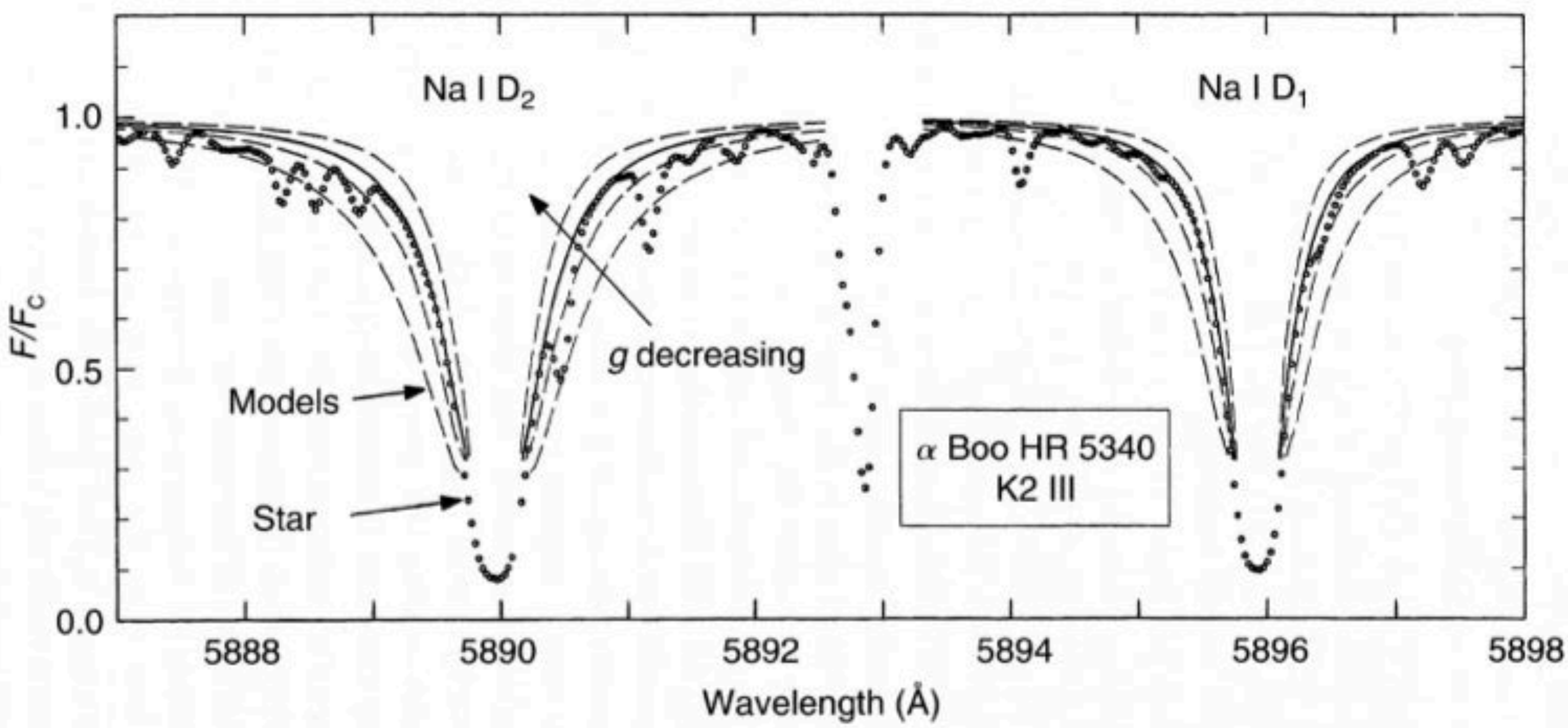

Fig. 15.3. The gravity dependence of the Na D lines is shown for models (lines) having $S_0 = 0.773$ and $\log g = 3.48$, 3.00, 2.60, and 2.00. The dots are the spectrum of Arcturus from Hinkle *et al.* (2000), but only every fourth point is plotted to avoid crowding. The pressure-broadened wings are matched well by the models, but notice how blended the stellar spectrum is, making it difficult to locate the Na line wings. The situation is actually worse than it appears because Hinkle *et al.* have already removed the numerous telluric lines that appear in this region.

Other strong lines: Ca I 6162

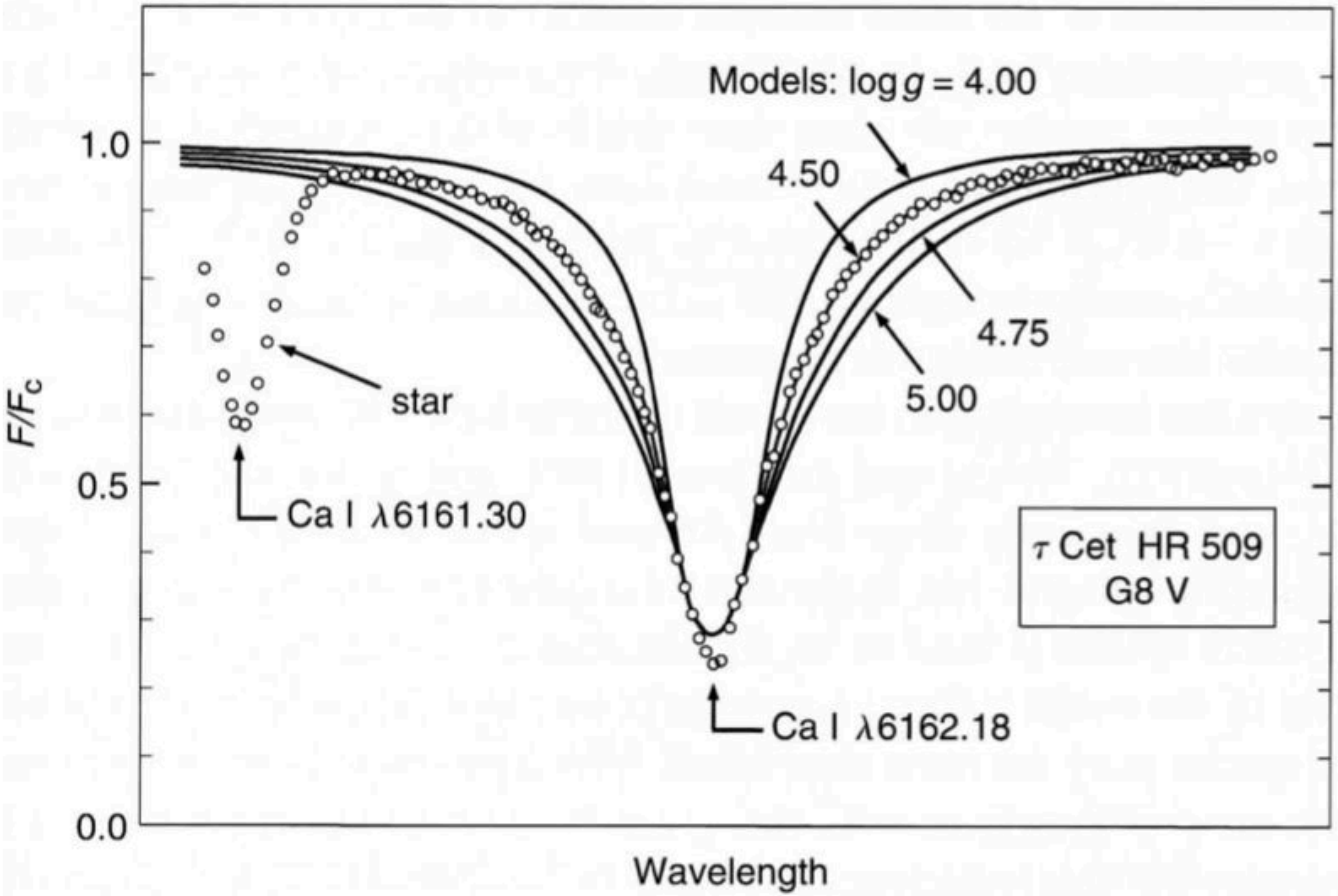

Fig. 15.4. Strong lines like this Ca I λ6162 line can be used to measure surface gravity. These models indicated the surface gravity of τ Cet to be near log $g = 4.50$. Data from Smith and Drake (1987).

Gray (2005)

$$A_X = \log\left(\frac{n_X}{n_H}\right) + 12$$

Chemical abundance

$$[X/H] \equiv \log\left(\frac{n_X}{n_H}\right)_\star - \log\left(\frac{n_X}{n_H}\right)_\odot$$

Abundance ratio relative to the Sun

$$[X/Fe] \equiv [X/H] - [Fe/H]$$

Abundance ratio relative to iron

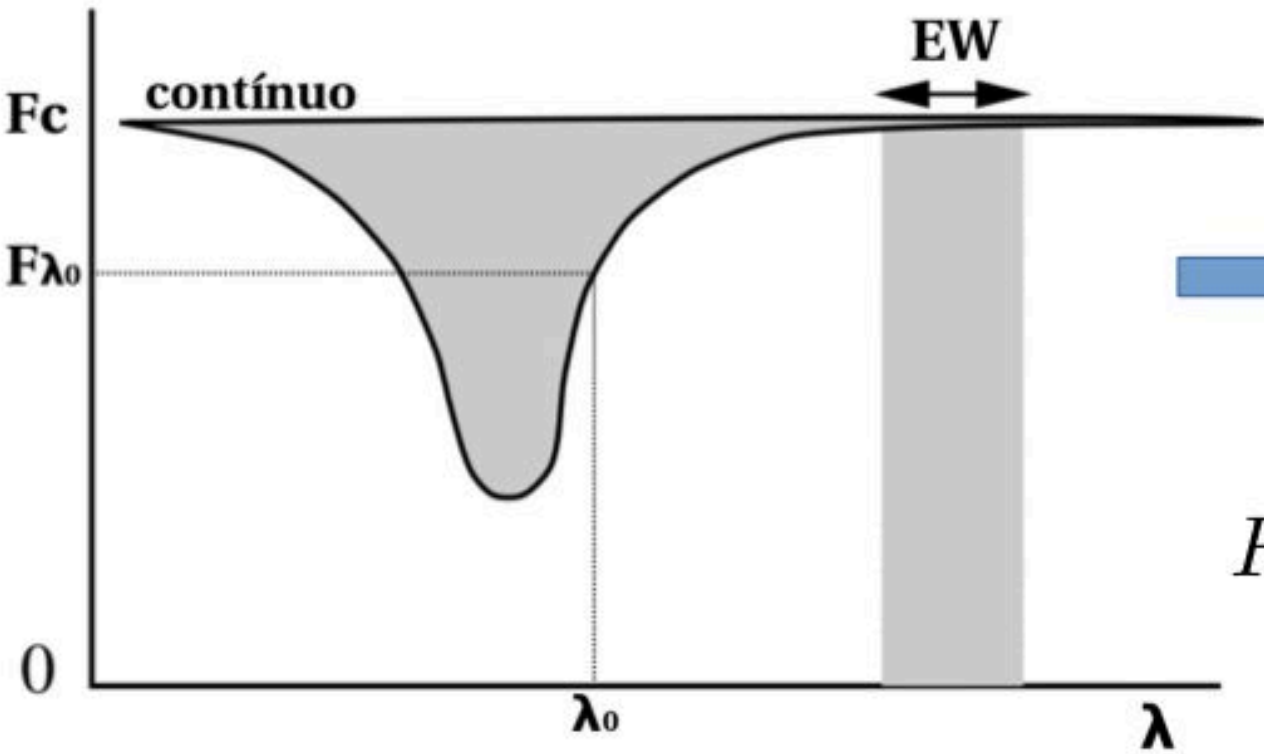

Equivalent width

$$EW = \int_0^\infty \left(1 - \frac{F_\lambda}{F_c}\right) d\lambda$$

$$F_\lambda(\tau_\nu = 0) = 2\pi \int_0^\infty B_\nu(T) E_2(\tau_\nu) d\tau_\nu$$

$$\log(EW/\lambda) = B + A_X + \log(gf) + \log\lambda - \theta\chi_{exc} - \log\kappa_{cont,\lambda}$$

Reduced equivalent width

Slide: Jhon Yana Galarza

Spectrum synthesis: 5577 A [OI] line

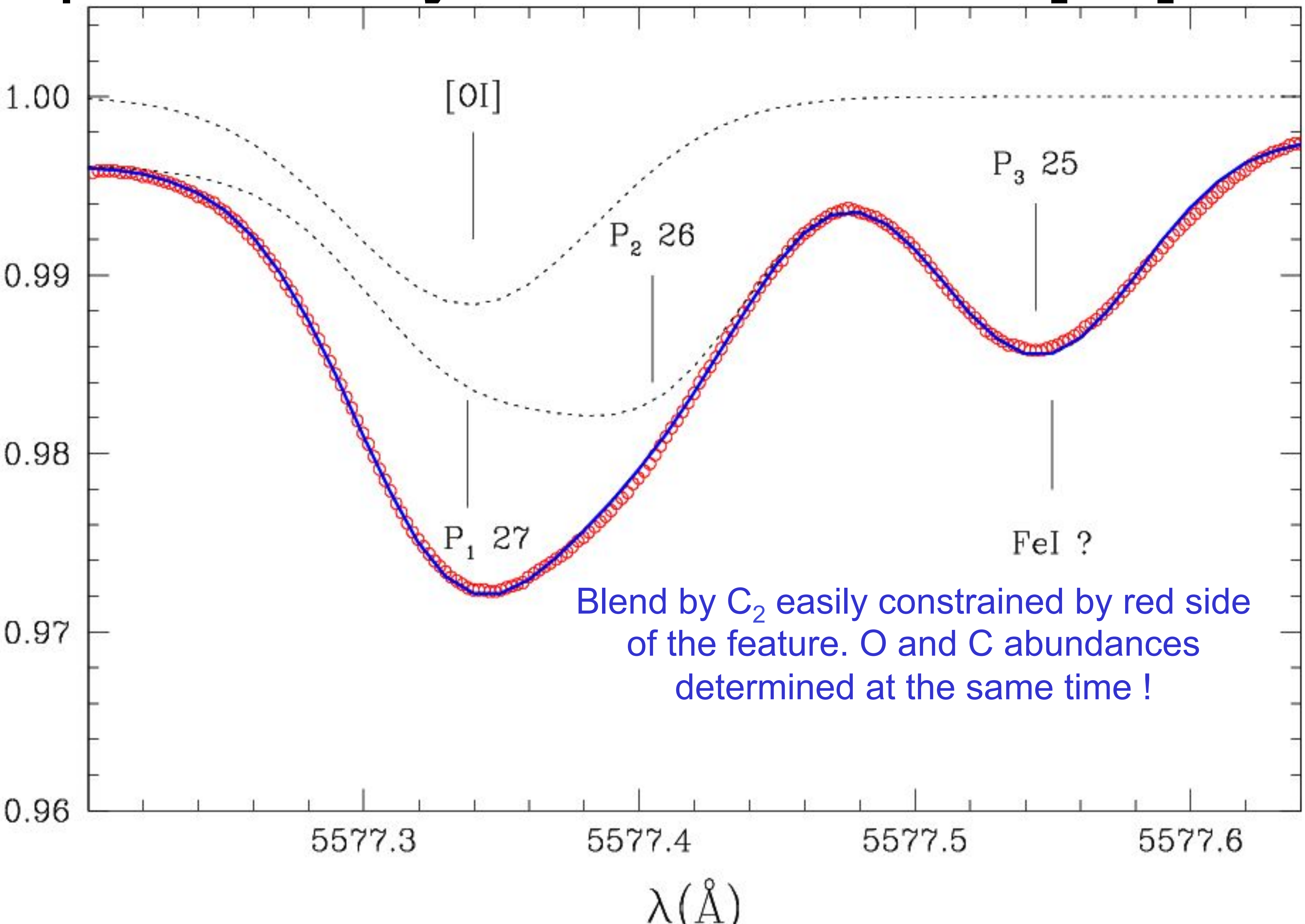

Blend by C_2 easily constrained by red side of the feature. O and C abundances determined at the same time !

Melendez & Asplund (2008).

Spectrum Synthesis of lithium in the Sun

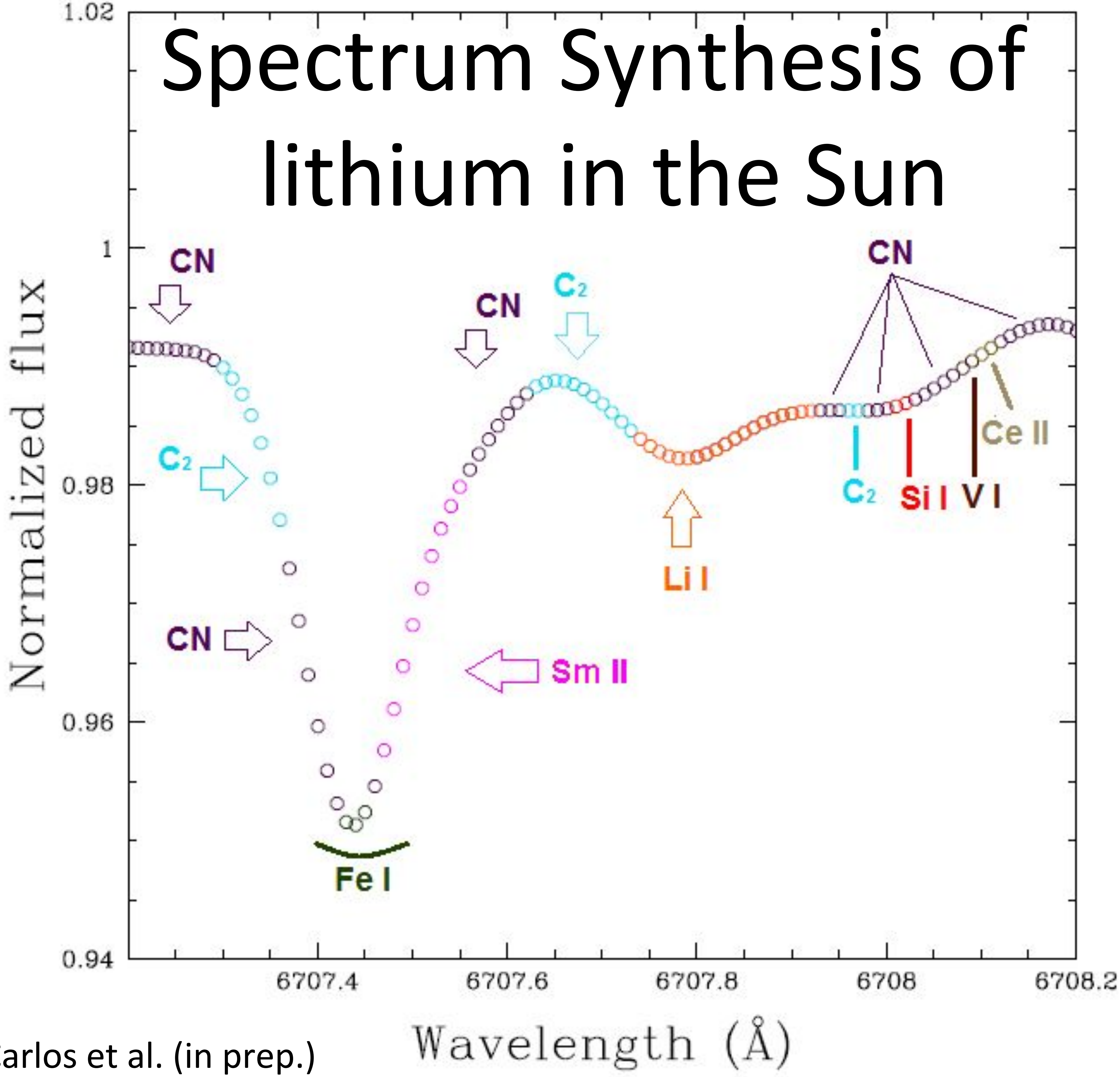

Marília Carlos et al. (in prep.)

Periodic Table of the Elements

- hydrogen
- alkali metals
- alkali earth metals
- transition metals
- poor metals
- nonmetals
- noble gases
- rare earth metals

1 H																	2 He
3 Li	4 Be											5 B	6 C	7 N	8 O	9 F	10 Ne
11 Na	12 Mg											13 Al	14 Si	15 P	16 S	17 Cl	18 Ar
19 K	20 Ca	21 Sc	22 Ti	23 V	24 Cr	25 Mn	26 Fe	27 Co	28 Ni	29 Cu	30 Zn	31 Ga	32 Ge	33 As	34 Se	35 Br	36 Kr
37 Rb	38 Sr	39 Y	40 Zr	41 Nb	42 Mo	43 Tc	44 Ru	45 Rh	46 Pd	47 Ag	48 Cd	49 In	50 Sn	51 Sb	52 Te	53 I	54 Xe
55 Cs	56 Ba	57 La	72 Hf	73 Ta	74 W	75 Re	76 Os	77 Ir	78 Pt	79 Au	80 Hg	81 Tl	82 Pb	83 Bi	84 Po	85 At	86 Rn
87 Fr	88 Ra	89 Ac	104 Unq	105 Unp	106 Unh	107 Uns	108 Uno	109 Une	110 Unn								

58 Ce	59 Pr	60 Nd	61 Pm	62 Sm	63 Eu	64 Gd	65 Tb	66 Dy	67 Ho	68 Er	69 Tm	70 Yb	71 Lu
90 Th	91 Pa	92 U	93 Np	94 Pu	95 Am	96 Cm	97 Bk	98 Cf	99 Es	100 Fm	101 Md	102 No	103 Lr

Solar Abundances from Asplund et al. (2009)